BMC Plant Biology

RESEARCH

Open Access

Unraveling the genetic basis of heat tolerance and yield in bread wheat: QTN discovery and Its KASP-assisted validation

Latief Bashir[1], Neeraj Budhlakoti[2], Anjan Kumar Pradhan[3], Azhar Mehmood[4], Mahin Haque[1], Sherry R. Jacob[1], Rakesh Bhardwaj[1], Kiran Gaikwad[4], Dwijesh Chandra Mishra[2], Satinder Kaur[5], Pradeep Kumar Bhati[6], G. P. Singh[1] and Sundeep Kumar[1*]

Abstract

Background Wheat (*Triticum aestivum* L.), a globally significant cereal crop and staple food, faces major production challenges due to abiotic stresses such as heat stress (HS), which pose a threat to global food security. To address this, a diverse panel of 126 wheat genotypes, primarily landraces, was evaluated across twelve environments in India, comprising of three locations, two years and two growing conditions. The study aimed to identify genetic markers associated with key agronomic traits in bread wheat, including germination percentage (GERM_PCT), ground cover (GC), days to booting (DTB), days to heading (DTHD), days to flowering (DTFL), days to maturity (DTMT), plant height (PH), grain yield (GYLD), thousand grain weight (TGW), and the normalized difference vegetation index (NDVI) under both timely and late-sown conditions using 35 K SNP genotyping assays. Multi-locus GWAS (ML-GWAS) was employed to detect significant marker-trait associations, and the identified markers were further validated using Kompetitive Allele Specific PCR (KASP).

Results Six ML-GWAS models were employed for this purpose, leading to the identification of 42 highly significant and consistent quantitative trait nucleotides (QTNs) under both timely and late sown conditions, controlled by 20 SNPs, explaining 3–58% of the total phenotypic variation. Among these, noteworthy QTNs were a major grain yield QTN (qtn_nbpgr_GYLD_3B) on chromosome 3B, a pleiotropic SNP AX-95018072 on chromosome 7A influencing phenology and NDVI, and robust TGW QTNs on chromosomes 2B (qtn_nbpgr_TGW_2B), 1A (qtn_nbpgr_TGW_1A), and 4B (qtn_nbpgr_TGW_4B). Furthermore, annotation revealed that candidate genes near these QTNs encoded stress-responsive proteins, such as chaperonins, glycosyl hydrolases, and signaling molecules. Additionally, three major SNPs AX-95018072 (7A), AX-94946941 (6B), and AX-95232570 (1B) were successfully validated using KASP assay.

Conclusion Our study effectively uncovered novel QTNs and candidate genes linked to heat tolerance and yield-related traits in wheat through an extensive genetic approaches. These QTNs not only corresponded with previously identified QTLs and genes associated with yield traits but also highlighted several new loci, broadening the existing genetic understanding. These findings provide valuable insights into the genetic basis of heat tolerance in wheat and offer genomic resources, including validated markers that could accelerate marker-assisted breeding and the development of next-generation heat-resilient cultivars.

Keywords Wheat, Heat stress tolerance, Yield related traits, SNPs, QTNs, ML-GWAS, KASP validation

*Correspondence:
Sundeep Kumar
Sundeep.Kumar@icar.gov.in
Full list of author information is available at the end of the article

Introduction

Wheat (*Triticum aestivum* L.) is one of the most widely cultivated cereal crops globally, serving as a staple source of food for the majority of the world's population. It accounts for approximately 20% of the total dietary calories and protein consumed worldwide [1]. However, the increasing prevalence of abiotic stresses, particularly heat stress, poses a significant threat to wheat production and global food security. Heat stress can adversely impact various growth stages of wheat, leading to reduced grain yield, quality, and economic returns [2, 3]. This challenge is further exacerbated by the effects of climate change, which is projected to intensify the frequency and severity of heat stress events in many wheat-growing regions worldwide [4–7]. Climate models predict a potential rise in average ambient temperature beyond 1.5 °C by the end of the twenty-first century (IPCC report 2022). Wheat thrives best when temperatures during the flowering (anthesis) and grain-filling stages remains within the optimal range of 12–22 °C. Exposure to temperatures outside this range can significantly reduce grain quality and yield [3, 8–11]. Terminal heat stress, occurring when the mean temperature during grain filling exceeds 31 °C, can lead to yield reductions of approximately 3–4% for each 1 °C increase above 28 °C [12, 13]. The impact of heat stress on wheat is multifaceted, affecting various physiological and biochemical processes. During the reproductive and grain-filling stages, heat stress can cause severe yield reductions by hampering pollen viability, fertilization, and grain development [2, 14, 15]. High temperatures can also accelerate phenological development, leading to a shorter grain-filling period and ultimately reducing grain weight and yield [16, 17]. Additionally, heat stress can disrupt photosynthesis, alter membrane stability, and induce oxidative stress, further compromising plant growth and productivity [18, 19].

Developing heat-tolerant wheat varieties is an important strategy for mitigating the detrimental effects of heat stress and ensuring sustainable wheat production to meet the ever increasing global food demand [16, 20, 21, 22]. Genetic improvement through marker-assisted breeding and the exploitation of genetic diversity present in wheat germplasm collections offer promising avenues for enhancing heat tolerance [23, 24]. With the advent of next-generation sequencing, advanced genotyping techniques like genotyping by sequencing (GBS) [25], high-throughput phenotyping [26], and advanced bioinformatics tools and packages [27], identifying and mapping genetic resources to specific traits of interest in various crops has become feasible.

Genome-wide association studies (GWAS) have become a powerful tool for dissecting complex traits and identifying quantitative trait nucleotides (QTNs) across various crop species, including wheat [28–33]. GWAS leverages linkage disequilibrium (LD) within diverse germplasm collections to pinpoint genetic markers linked to traits of interest [34–36]. Single-locus GWAS (SL-GWAS) methods detect single-marker associations but often miss important loci with smaller effects, despite corrections like the Bonferroni adjustment [37]. To overcome these limitations, multi-locus GWAS (ML-GWAS) models, such as mrMLM, FASTmrMLM, FASTmrEMMA, pKWmEB, pLARmEB, and ISIS EMBLASSO have been developed [38–43]. These models consider the combined effects of multiple loci, offering higher statistical power and lower false-positive rates. Recent Studies have demonstrated that ML-GWAS improves the detection of marker-trait associations (MTAs) and provides greater insights into the genetic basis of complex traits compared to traditional SL-GWAS methods [44–48].

The identification of genomic regions associated with terminal heat tolerance using the LD mapping approach remains crucial, particularly when examining naturally occurring variations in landraces and locally adapted wheat cultivars. This necessity arises from the highly complex nature of heat tolerance, where QTNs identified for specific locations or environments may not be universally applicable across different environments [49]. In other words, the genetic markers associated with heat tolerance in one environment or region may not confer the same level of tolerance in another environment due to the intricate interplay between genotype and environmental factors.

The validation of identified QTNs and associated markers is a critical step in confirming their utility for marker-assisted selection and breeding applications. Marker validation ensures the reliability and robustness of the identified associations and assesses their transferability across different genetic backgrounds and environments. The KASP marker system has emerged as a cost-effective and flexible genotyping platform for marker validation and application in breeding programs [50–53]. KASP markers use allele-specific oligo extension and fluorescence resonance energy transfer (FRET) for signal generation, allowing for accurate and high-throughput genotyping [54]. The KASP approach has been successfully employed for marker validation and marker-assisted selection in various crop species, including wheat [50, 53, 55–58].

This study was conducted with the aim of mapping and validating genomic regions and QTNs associated with yield-related traits in wheat under both timely and late-sown conditions, which subject the crop to heat stress. A diverse panel of wheat genotypes, primarily from Indian wheat germplasm, was utilized. Identifying these genomic regions is crucial, as they offer potential targets

for breeders working to develop heat-tolerant wheat lines. As climate change leads to more frequent and intense heat stress events, the development of heat-resilient wheat varieties becomes increasingly important for sustaining production and ensuring global food security.

Materials and methods

Germplasm and phenotyping

Out of the 600 wheat germplasm lines evaluated for yield related traits, 126 diverse genotypes were selected for phenotypic assessment on the basis of their superior agronomic performance. The association panel mainly consists of landraces and exotic collections identified at the ICAR-National Bureau of Plant Genetic Resources (ICAR-NBPGR), New Delhi (Table S1). Phenotypic evaluation was conducted across multiple locations managed by the Borlaug Institute for South Asia (BISA) in India, including the BISA farm at Pusa, Bihar (25.9599^{O}N, 85.6696^{O}E, North East Plain Zones, NEPZ), BISA farm at Jabalpur, Madhya Pradesh (23.2241^{O}N, 80.0709^{O}E, Central Zone, CZ), and BISA farm at Ludhiana, Punjab (31.267^{O}N, 75.7686^{O}E, North West Plain Zones, NWPZ). The trials spanned two consecutive crop seasons, 2020–2021 & 2021–2022, with each season comprising two sowing regimes: normal sowing in mid-November under non-stress conditions, and late sowing in mid-December to induce heat stress. Overall, the evaluation covered twelve different environments, incorporating all combinations of growing conditions, locations, and years.

The evaluation of selected genotypes for heat tolerance was conducted based on the first and second year trial results across all environments. The experimental design implemented an alpha lattice arrangement, with each plot measuring 3.024 square meters (2.8 m × 1.08 m). Each plot consisted of six rows with a row-row spacing of 18 cm. Five check varieties, namely RAJ3765 (CK1), DBW107 (CK2), DBW71 (CK3), HD2932 (CK4), and PBW771 (CK5), were utilized throughout the experiment. Maximum and minimum temperatures were recorded at various wheat growth stages under both sowing regimes. Standard agronomic practices were adhered to throughout the crop season. Disease management included two applications of the systemic fungicide Tilt (Propiconazole 25% EC), administered at 40–45 days and 70–75 days after sowing. Harvesting was carried out in the first week of April for the normal sown crop and in the first week of May to the second week of May, depending on crop maturity and environmental conditions for the late-sown crop. Threshing was performed mechanically to separate seeds from the plants. These procedures were consistently applied across both crop seasons (2020–2021 and 2021–2022). For field data recording, the following instruments were utilized: (i) MultispeQ v2.0 for measuring agronomical, phenological, and yield component traits, (ii) Infrared thermometer for canopy temperature measurement, (iii) GreenSeeker crop sensor for ground cover assessment, and (iv) electronic balance for weighing grains. A total of 3024 samples (126 genotypes × 2 replications × 2 conditions × 3 locations × 2 years) were collected for the final evaluation.

Data collection adhered to the standard procedures outlined in the manual "Wheat Physiological Breeding II: A Field Guide to Wheat Phenotyping" [59]. The following 12 traits were measured: (i) Germination percentage (GERM_PCT): number of germinated seedlings was recorded in percentage at 55DAS (ii) Early ground cover (E_CG): Recorded as percentage at 80DAS (iii) Ground cover (GC): Ground cover was measured in percentage 95DAS (iv) Days to Booting (DTB): Recorded as the number of days from the date of sowing to booting stage of wheat (v) Days to Heading (DTHD): Recorded as the number of days from the date of sowing to the heading stage of wheat (vi) Days to Flowering (DTFL): Recorded as number of days from the date of sowing when 75% plants were in heading (vii) Days to Maturity (DTMT): Recorded as number of days from the date of sowing when 90% plants are ready for harvest i.e., at the physiological maturity (viii) Plant Height (PH): Measured at physiological maturity in centimeters (cm) on main tiller from the ground level to the tip of spike excluding awns at the maturity on 5 plants (ix) Grain Yield (GYLD): Measured as grams per plot (gm/plot) and tons per hectare (t/ha) and recorded from one meter row length. It was (x) Thousand Grain Weight (TGW): Measured as weight of 1000 randomly selected grains (average of 5 observations) in grams through electronic balance (xi) Normalized Difference Vegetation Index (NDVI): NDVI was recorded at all five stages of growth i.e., at ground cover, heading, anthesis, grain filling and maturity and recorded using GreenSeeker crop sensor and (xii) Canopy Temperature (CT): CT was recorded also measured at five growth stages using Infrared thermometer.

Statistical analysis of phenotypic traits

To assess the significance of phenotypic data across various environments, an Analysis of Variance (ANOVA) was conducted using SAS v9.4. The interrelationships among yield-related traits were examined through Pearson correlation analysis. To better understand the distribution of phenotypic values for the traits, Best Linear Unbiased Estimates (BLUEs) were computed for each trait. Principal component analysis (PCA) was also conducted for all traits under both timely and late sown conditions. Furthermore, to determine genotype stability, superiority, and identify the optimal genotypes for specific traits under heat stress conditions, genotype

and genotype-by-environment (GGE) biplot analysis and was performed using the R program [60, 61]. Additionally, the broad-sense heritability of the traits was determined using the restricted maximum likelihood (REML) method by following the approach of Gilmour et al. (1995) [62], accounting for genotype by environment interactions. All these analysis was computed by R Statistical Software (v4.1.2; R Core Team 2022).

Genotyping and SNP variant calling

Genomic DNA was extracted using the CTAB method [63] from approximately 300 mg of leaf tissue from 15-day-old seedlings. The quality of the DNA was assessed using a NanodropTM 2000 (Thermo Fisher Scientific, Wilmington, DE, USA), and only high-quality DNA samples were selected for genotyping. The genotyping was performed using the 35 k Axiom® Wheat Breeders Array, following the procedure outlined by Affymetrix (Axiom® 2.0 Assay for 294 samples, P/N 703, 154 Rev. 2). Further to ensure reliable data, SNP markers with > 10% missing data, < 10% MAF, and those with monomorphic alleles were excluded from the analysis. A total of 15,805 polymorphic SNPs markers were utilized for association mapping and other downstream analyses.

Population structure, kinship and LD analysis

The population structure was determined using a model-based clustering approach implemented in STRUCTURE v2.3.4 [64]. Ten iterations of STRUCTURE were performed for each specified K, with parameters including a burn-in period of 20,000 and 50,000 Markov Chain Monte Carlo (MCMC) iterations after burn-in. The best-fit number of clusters was determined using adhoc statistics ΔK [65], which was facilitated by 'Structure Harvester', a web-based tool [66]. Additionally, a kinship matrix though NJ tree was also estimated using Tassel v5.0 [67], for aiding the GWAS analysis.

LD between markers was assessed using TASSEL v5.0 [67], with significance determined through 1000 permutations. Background LD in the wheat AM panel was calculated to establish the critical distance for LD decay using R. LD decay distance across sub-genomes and the whole genome was estimated by plotting LD r^2 values against inter-SNP physical distance. The critical r^2 value indicating true physical linkage was determined using the 95th percentile of transformed r^2 data of unlinked markers [28]. The intersection of the LD decay curve occurred at $r^2 = 0.17$, serving as the background threshold for LD.

Association analysis

Most single-locus GWAS (SL-GWAS) methods rely on identifying single-marker associations in genome-wide scans, while accounting for population structure and polygenic background. To reduce false positives, the Bonferroni correction for multiple testing is often applied [37]. However, this approach requires repeated adjustments to critical values and overlooks the combined effects of multiple loci, frequently resulting in the exclusion of important quantitative trait loci (QTLs) with smaller effects. To address these limitations, multi-locus GWAS (ML-GWAS) models have been developed. ML-GWAS models offer several advantages over single-locus approaches, including improved statistical power to detect small-effect variants and better accounting for linkage disequilibrium and epistatic interactions. These models reduce false-positive rates by considering multiple markers simultaneously enhance the ability to explain missing heritability by capturing cumulative effects of multiple loci. Association analyses were conducted using six ML-GWAS models: mrMLM [38], FASTmrMLM [39], FASTmrEMMA [40], pKWmEB [41], pLARmEB [42], and ISIS EM-BLASSO [43]. These six models were implemented using the R package mrMLM v4.0 (https://cran.r-project.org/package=mrMLM) with default settings. A threshold with a LOD score of ≥ 3.00 was applied to identify significant QTNs for downstream analysis and interrogation.

Marker identification and their functional annotations

In this study, we identified QTNs across all twelve environments. To ensure precision in identifying heat stress-related QTNs, we focused specifically on those that were consistently identified under both normal sowing and heat stress conditions. More precisely, we included only those QTNs that were detected in at least four environments, with at least three of those environments being heat stress conditions (late sowing). Furthermore, to increase the reliability of our findings, only those QTNs that were identified by five out of the six ML-GWAS models were taken into consideration. This rigorous methodology ensured that the identified QTNs were robust and consistently associated with heat stress tolerance while also taking into account their behavior in normal conditions for a more comprehensive understanding. In the GWAS analysis, QTNs identified by at least two GWAS models were considered reliable associations. The total number of QTNs detected by at least two models was further categorized. QTNs identified by at least three models within a single location/environment were deemed significant. Those detected by five out of six models across four or more environments were classified

as highly significant and consistent QTNs. This classification facilitated the evaluation of allele performance in relation to yield related traits under different environments. A Manhattan plot was generated to visualize the LOD scores and statistical significance of marker-trait associations across chromosomes, highlighting highly significant and consistent QTNs. Additionally, to investigate the genetic potential of genes linked to these QTNs and compare our results with previous studies, a physical map of wheat chromosomes was constructed using MapChart 2.3 (https://www.wur.nl/en/show/Mapchart.htm), illustrating the SNPs and their respective genomic positions. Furthermore, highly significant and consistent QTNs were annotated to identify potential candidate genes. These QTNs were compared against the *Triticum aestivum* genome assembly IWGSC-refseq version 1.0 using the online resource Ensembl Plants (https://plants.ensembl.org/Triticum_aestivum/Tools/Blast). Additionally, to cross-validate the results obtained from Ensemble Plants, the DAVID online tool (https://david.ncifcrf.gov/summary.jsp) was employed, offering functional annotation and Gene Ontology (GO) for the identified genes. Highly significant and consistent QTNs were prioritized, as they were considered more reliable and expected to perform well across diverse environments. This approach aimed to identify robust associations between genomic regions and yield-related traits in wheat under heat stress.

Validation of identified QTNs

To validate the QTNs, KASP markers were developed using highly significant and consistent SNPs. The KASP Assay workflow was conducted in Wheat Molecular Biology Lab, school of agricultural biotechnology, Punjab Agricultural University, Ludhiana, India. To design markers for the identified SNPs, a 100 bp sequence surrounding each SNP was extracted from the wheat reference genome (IWGSC RefSeq version 2.1). Primers for the KASP markers were then designed using the Polymarker tool (doi:https://doi.org/10.1093/bioinformatics/btv069). Two allele-specific forward primers were labeled with FAM (5'-GAAGGTGACCAAGTTCATGCT-3') and HEX (5'-GAAGGTCGGAGTCAACGGATT-3'), while the reverse primer remained unlabeled. PCR reactions were set up in a 4 µl volume, consisting of 2 µl genomic DNA (30 ng/µl), 1.96 µl 2X KASP reaction mix, and 0.04 µl KASP assay mix containing the primers. The reactions were run in a 384-well plate using an Applied Biosystems Veriti thermocycler. The thermal cycling conditions included an initial denaturation at 95 °C for 15 min, followed by 10 touchdown cycles of 95 °C for 10 s and 61–57 °C for 1 min (with a 0.6 °C decrease per cycle), and finally 25 cycles of 95 °C for 20 s and 57 °C for 1 min for annealing. The primers for the KASP assays were ordered from Barcode Biosciences (www.barcodebiosciences.com). The genotypic data from the homozygous alleles were analyzed using the Kruskal–Wallis test to identify statistically significant differences between the alleles (Figure S7) [68].

Results

Phenotyping and correlation analysis

The ANOVA results for yield-related traits revealed significant differences ($p \leq 0.0001$) across genotype, location, year, and growth conditions (Table 1). Additionally, the BLUE value indicated that several yield-related parameters, including GERM_PCT, GC, DTB, DTHD, DTFL, DTMT, PH, GYLD, TGW, GC_NDVI, H_NDVI, AN_NDVI, GF_NDVI, and MT_NDVI, significantly reduced under late-sown conditions. Conversely, traits such as E_GC, H_CT, AN_CT, GF_CT, and MT_CT enhanced under heat stress conditions (Table S2a & S2b). Furthermore, crops sown on time (in November) experienced a maximum canopy temperature of ≥ 23.41 °C and a minimum of ≤ 19.74 °C during anthesis. During the grain filling stage, the canopy temperature peaked at ≥ 34.65 °C and dipped to ≤ 27.75 °C. For late-sown wheat, the maximum CT at anthesis was ≥ 32.5 °C and the minimum was ≤ 23.9 °C. However, during the grain filling stage, there was a sharp increase in average temperature, with maximum CT reaching ≥ 40.8 °C and minimum CT dropping to ≤ 21.1 °C, subjecting the wheat crop to severe heat stress. As a result, grain yields were lower in late-sown trials aimed at studying heat stress compared to those sown on time.

The Effect of HS on yield traits was most pronounced in Samastipur (Bihar), followed by Ludhiana (Punjab) and Jabalpur (Madya Pradesh). Moreover, mean grain yield was highest in Jabalpur (4.69–5.70 t/hac) followed by Ludhiana (3.01–5.45 t/hac) and Samastipur (1.89–5.0 t/hac) (Table S3-a, S3-b, S3-c & S3-d; S4-a, S4-b, S4-c & S4-d; S5-a, S5-b, S5-c & S5-d).

Further results of correlation analysis i.e. Pearson's correlation coefficient, is calculated and presented for both under timely and late sown regimes (Figs. 1a and b). A significant positive correlation between GC and DTB ($r = 0.32$), DTHD ($r = 0.32$), DTFL ($r = 0.32$), DTMT ($r = 0.29$) and PH ($r = 0.38$) was seen under timely sown conditions. DTB also showed a strong positive correlation with DTHD ($r = 0.91$), DTFL ($r = 0.99$), DTMT ($r = 0.86$), and PH ($r = 0.49$). In contrast, GYLD exhibited a significant negative correlation with DTB ($r = -0.52$), DTHD ($r = -0.44$), DTFL ($r = -0.47$), DTMT ($r = -0.48$), and PH ($r = -0.52$). Additionally, there was a strong negative association between TGW and DTB ($r = -0.37$), DTHD ($r = -0.37$), DTFL ($r = -0.38$), and DTMT

Table 1 ANOVA of yield related traits in bread wheat evaluated under timely and late sown conditions

Source	DF	GERM_PCT	E_GC	GC	DTB	DTHD	DTFL	DTMT	PH	GYLD	TGW
Genotype	125	318.56***	117.59 NS	99.13 NS	1389.10***	1320.64***	1198.34***	379.08***	4491.52***	11.23***	216.25***
Location	2	18524.98***	221288.03***	66842.65***	183281.56***	197003.98***	195022.99***	108468.10***	27789.55***	1150.77***	12612.11***
Year	1	22603.66***	7.60 NS	45384.94***	3346.29***	2985.49***	3823.49***	2173.51***	20572.70***	22.09***	2312.01***
Condition	1	7075.92***	64568.13***	37429.87***	37376.90***	61737.10***	92937.90***	352725.21***	32704.24***	1526.97***	41046.69***
Replication	1	192.35 NS	210.36 NS	137.69 NS	4.66 NS	6.12 NS	11.55 NS	47.99 NS	1.52 NS	5.85 NS	14.69 NS
Error	2892	100.37	94.38	101.75	37.3156	37.23	37.25	23.94	143.95	1.25	45.28
Source	**DF**	**GC_NDVI**	**H_NDVI**	**AN_NDVI**	**GF_NDVI**	**MT_NDVI**	**H_CT**	**AN_CT**	**GF_CT**	**MT_CT**	
Genotype	125	0.008 NS	2.11***	2.79***	2.73***	1.65***	12.56***	776.25 NS	6.00 NS	22.88***	
Location	2	0.05 NS	45.41***	0.07***	473.34***	9.75***	4957.28***	2053.20 NS	9580.93***	5533.46***	
Year	1	2.40***	206.64***	690.79***	203.04***	17.50***	181.24***	1173.14 NS	3113.21***	137.05***	
Condition	1	86.49***	0.55	634.45***	1045.56***	62.39***	27450.65***	21564.65***	29698.04***	11546.58***	
Replication	1	0.00 NS	0.11 NS	0.02 NS	0.99 NS	1.00 NS	0.70 NS	727.09 NS	0.26 NS	1.64 NS	
Error	2892	0.007	0.003	0.006	0.01	0.07	5.65	744.51	14.60	12.85	

DF Degree of freedom, *NS* Non-significant

*** indicates < 0.0001 level of significance

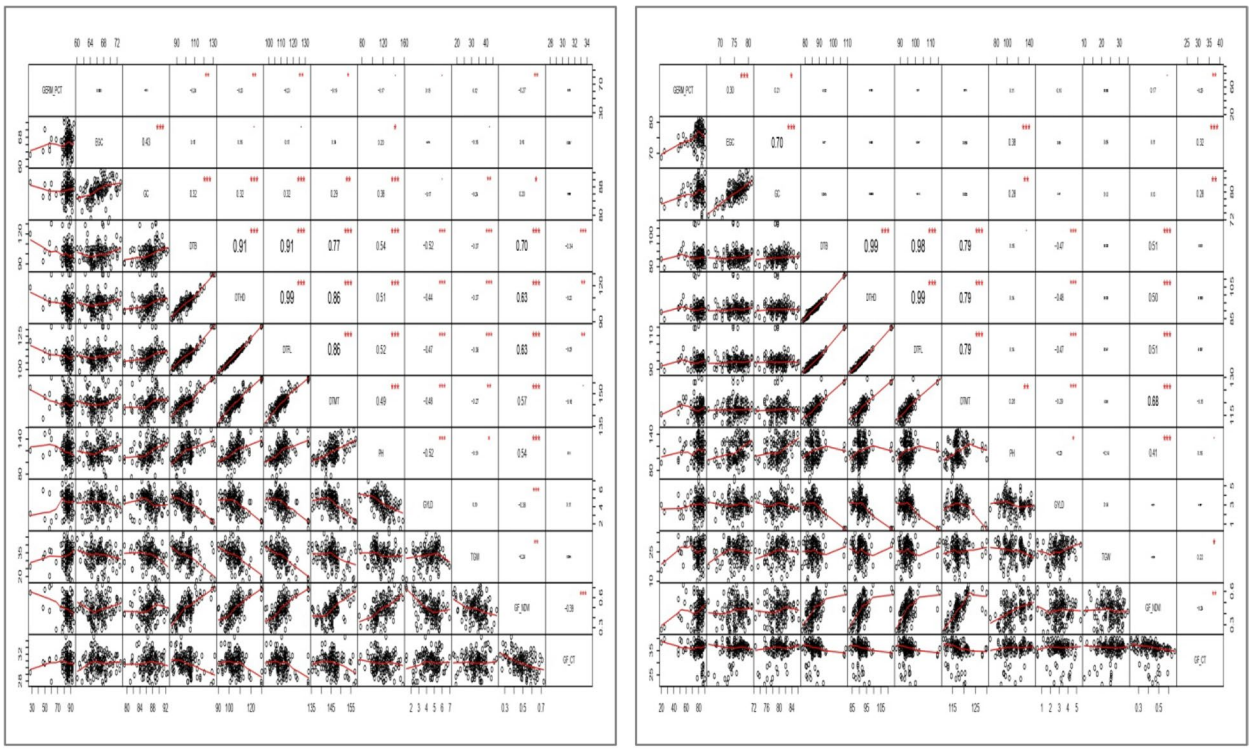

Fig. 1 Correlation matrix that can be read from the diagonal for all pairs of the observed yield related traits in bread wheat. Every potential pairing is shown in the lower panel using scatter plots and smoothing splines, and the matching Pearson's correlation coefficient is shown in the upper panel with text size based on absolute value. In the upper panel, the *p*-value obtained after testing the correlation coefficient against the null hypothesis is symbolically encoded at the levels of 0.1 ('), 0.05 (*), 0.01 (**), and 0.001 (***). **a** Timely sown, (**b**) Late sown

($r=-0.27$). The association between GYLD and TGW was positive ($r=0.10$). In contrast, TGW and GYLD were the only traits that showed a positive association with GF_CT.

All traits followed the same pattern under late-sown conditions as they did under timely-sown ones, except for GYLD, which shows a negative correlation with GF_CT ($r=-0.067$). However, the strength of correlations between traits varies when compared to the timely sown conditions (Figs. 1a and b). Additionally, the broad-sense heritability values for the traits GERM_PCT, E_GC, GC, DTB, DTHD, DTFL, DTMT, PH, GYLD, TGW, GC_NDVI, H_NDVI, AN_NDVI, GF_NDVI, MT_NDVI, H_CT, AN_CT, GF_CT, and MT_CT were found to be 0.87, 0.74, 0.78, 0.77, 0.84, 0.81, 0.92, 0.91, 0.79, 0.88, 0.74, 0.83, 0.84, 0.76, 0.78, 0.72, 0.85, 0.93, 0.82, and 0.72, respectively, suggesting that most of the phenotypic variation was due to genetic factors.

PCA & GGE biplot analysis

PCA was used to identify which measured parameter most accurately represented the response under stress conditions based on principal component scores The PCA results indicated that five factors had eigen values > 1 (Figure S1). Under timely sown conditions, the PCA biplot effectively differentiated wheat genotypes based on their heat stress response, with the first two principal components explaining 52.1% of the total phenotypic variation (PC1: 39.8%, PC2: 12.3%) (Figure S1a). PC1 primarily separated genotypes based on their physiological performance and heat adaptation mechanisms. Genotypes positioned on the positive axis of PC1 (IC394006, IC536741, IC284000) demonstrated strong associations with favorable heat-adaptive traits including higher NDVI values (MT_NDVI, GF_NDVI, AN_NDVI) and plant height (PH), suggesting their superior heat tolerance. Conversely, genotypes clustered on the negative PC1 axis (IC138428, EC573974, and IC290196) showed stronger associations with yield-related traits (GYLD) and canopy temperature measurements (MT_CT, GF_CT), indicating different stress-response mechanisms. PC2 further discriminated genotypes based on their early vigor and heat response characteristics. Genotypes in the positive PC2 direction (IC119814, IC130600) exhibited superior germination (GERM_PCT) and early ground cover (E_GC), while those in the negative direction

(IC542070, IC273330, IC534183) were associated with higher heat canopy temperature (H_CT) and lower NDVI values, suggesting heat susceptibility under timely sown conditions (Figure S1a).

Under late sown conditions, the first two principal components explained 50.1% of total phenotypic variation (PC1: 32.9%, PC2: 17.2%) (Figure S1b). PC1 distinctly separated genotypes based on their physiological responses and heat adaptation mechanisms, where genotypes positioned on the positive axis (IC394606, IC280872) exhibited strong associations with NDVI (MT_NDVI, GF_NDVI), DTB, DTHD, DTFL and plant height (PH), indicating superior heat tolerance. In contrast, genotypes clustered on the negative PC1 axis (IC138428, EC573974, and EC465070) showed stronger associations with yield-related traits (GYLD) and canopy temperature (CT), suggesting different stress-response strategies under late sown conditions (Figure S1b).

Genotypes in the positive PC2 direction (IC108637, IC130428) demonstrated superior germination (GERM) and early ground cover (E_GC), while those in the negative direction (IC290180, IC543165) were associated with higher heat canopy temperature (H_CT) and lower NDVI values, indicating potential heat susceptibility. The biplot revealed clear trait associations where early growth parameters (E_GC, GERM_PCT) clustered together, while NDVI measurements showed negative associations with canopy temperature traits. This clustering pattern identified four distinct groups under both timely and late sown conditions: heat-tolerant genotypes (upper right quadrant), yield-stable genotypes (left quadrants), heat-susceptible genotypes (lower quadrants), and balanced-performance genotypes (near origin) (Figure S1a & S1b).

Trait-wise GGE biplot analysis was conducted for yield component traits including GERM_PCT, E_CG, GC, DTB, DTHD, DTMT, PH, TGW, and GYLD to determine the top genotypes and their stability across twelve different environments (Figures S2a–d, S3a–d). For GERM_PCT, genotypes EC464070 and EC576792 emerged as the best performers across all environments. Genotypes IC111787, IC128416, and IC138426 were specifically well-suited for E_CG, while IC321853, EC576930, and IC262779 were identified as the top performers for GC across all environments. For DTB, EC313710 and EC187159 were the best-performing genotypes. In the case of DTHD, IC258214, EC573974, and IC258208 were the top performers, whereas IC128438, IC128416, and IC128640 excelled in DTMT. For PH, genotypes EC576792, EC576578, and IC258214 stood out, while IC258208, IC406688, and IC447520 were the best for TGW. Additionally, genotypes IC279335 and IC252668 were identified as promising for GYLD across all locations.

The mean vs. stability analysis results indicate that EC464070 had the highest mean value for GERM_PCT, followed by EC313710 and EC576792, all of which demonstrated consistent tolerance across diverse environments. The most stable genotypes for GERM_PCT, showing above-average performance, were IC138589, IC138600, and IC138637. Similarly, IC279878 and IC145522 exhibited stable and above-average performance for E_CG. For GC, genotypes EC464070 and EC57693 were stable and above average, while IC534929 and IC252429 showed stability and superior performance for DTB. The stable genotypes for DTHD were IC384533 and IC469480, and for DTMT, IC118722 and IC252469 were stable. Likewise, the most stable and above-average performing genotypes for PH and TGW were IC345589, IC531183, and IC469480, IC554661, respectively. For GYLD, the most stable genotypes with above-average performance were IC393128 and IC252469.

The ranking of genotypes based on GGE biplot analysis can be determined by measuring the distance from the ideal genotype. For GERM_PCT, EC464070 was identified as the most favorable genotype, followed by EC313710 (Figures S2a–d, S3a–d). Similarly, other genotypes can be ranked in descending order by their distance from the center of the circle. IC396619 was the most favorable genotype for E_CG, followed by IC574388, while IC336751 was the most suitable for GC. For DTB, IC252796A was identified as the most appropriate genotype, followed by IC321864 and IC321853. For DTHD, the top-ranked genotypes were IC128388 and IC443722. In the case of DTMT, IC128283, IC128388, and IC116276 were deemed the most suitable genotypes. For PH and TGW, IC574388, IC583383, and IC309875, IC82425A were identified as the most suitable, respectively. Finally, IC336751 was found to be the most suitable genotype for GYLD.

Genotyping and marker coverage

A 35 K Axiom SNP array was used in the genotyping of current wheat association panel, resulting in the identification of 35,143 SNPs. These SNPs were subsequently filtered based on various quality parameters, including MAF, monomorphic SNPs, and missing data. After filtering, 15,805 polymorphic SNPs were retained for association mapping and other downstream analysis. The average number of SNPs per chromosome was 752.6, ranging from 287 on chromosome 4D to 1,140 on chromosome 2B (Table 2). Sub-genome B had the highest number of polymorphic SNPs (6,113, 38.67%), followed by sub-genome A (5,096, 32.26%), and sub-genome D (4,596, 29.07%). The maximum number of SNPs in sub-genome A was found on chromosome 2A (940), followed by chromosome 1A (823). In sub-genome B,

Table 2 Chromosome wise distribution of polymorphic SNPs

CHR	No. of polymorphic SNPs	CHR	No. of polymorphic SNPs
1A	823	4D	287
1B	861	5A	718
1D	752	5B	1107
2A	940	5D	762
2B	1140	6A	610
2D	917	6B	836
3A	636	6D	621
3B	976	7A	811
3D	563	7B	746
4A	558	7D	694
4B	447	**Total**	**15,805**

chromosome 2B had the most SNPs (1,140), followed by chromosome 5B (1,107). For sub-genome D, chromosome 2D had the most SNPs (917), followed by chromosome 7D (694) (Tables S6-a, S6-b, & S6-c).

Population structure, diversity and LD analysis

To analyze the population structure of the association panel, relationship between the ΔK value and the varying number of hypothetical subgroups (K) is observed, which showed the peak ΔK value at K = 2, hence indicating the optimal number of subpopulations i.e. 2 Sub-groups (Figure S4). Consequently, the panel of 126 wheat genotypes was classified into two distinct subpopulations: SP1 and SP2 (Fig. 2a), of which 61 were assigned to subpopulation 1 (SP1), and 65 to subpopulation 2 (SP2). Among these, 81.66% of the genotypes were classified as pure lines (i.e., > 80% membership to SP1), with 16.4% being exotic collections (EC) and 83.6% indigenous collections (IC). The remaining 18.33% in SP1 were classified as admixtures. In SP2, 75% of the genotypes were pure lines (4.6% EC and 95.4% IC), while 25% were admixtures. The presence of two subpopulations has also been confirmed by phylogeny analysis through NJ tree (Fig. 2b).

LD between marker pairs was estimated as the squared allele frequency correlation (R^2) between intra-chromosomal SNPs with known chromosomal positions. To assess the significance of pair-wise LD, 1,000 permutations were performed at a probability level of 0.01 (Figure S5). The background LD in the wheat association mapping (AM) panel was calculated to identify the critical distance at which LD decays. To assess LD decay, LOESS (locally weighted linear regression) curves were fitted for each sub-genome and the entire genome. A threshold for LD decay was determined based on the convergence of the LD decay curve at $r^2 = 0.17$. LD decayed the fastest in sub-genome A, followed by sub-genomes D and B. Specifically, LD declined at 3.16 Mb in sub-genome A, compared to 3.18 Mb in sub-genome D and 4.81 Mb in sub-genome B (Figs. 3a-d). Overall, LD for the entire genome decayed at 3.75 Mb. Consequently, we selected a 1 Mb window size for candidate gene analysis, which was applied uniformly across all chromosomes (Figure S6). This window size was chosen to ensure that the candidate genes identified were within regions of the genome that exhibit sufficient genetic variation, as indicated by the LD decay pattern. The 1 Mb window provides a balance between capturing a reasonable number of genetic markers while maintaining the biological relevance of the candidate genes.

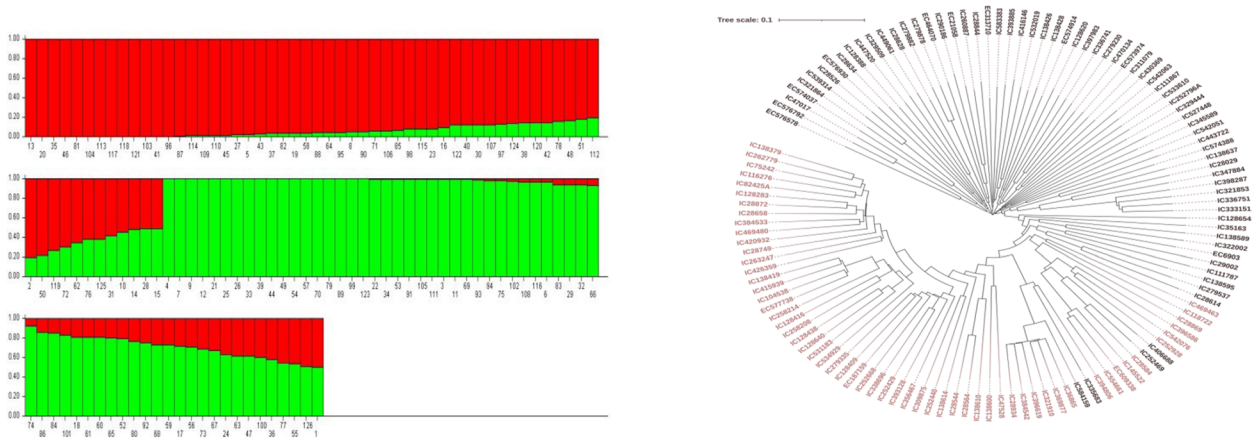

a **b**

Fig. 2 Population structure and kinship analysis: (**a**) Structure of the AM panel showing two subpopulations viz. SP1 (red, 61 genotypes), SP2 (green, 65 genotypes) (**b**) NJ tree showing genetic relationship among 126 wheat germplasm lines

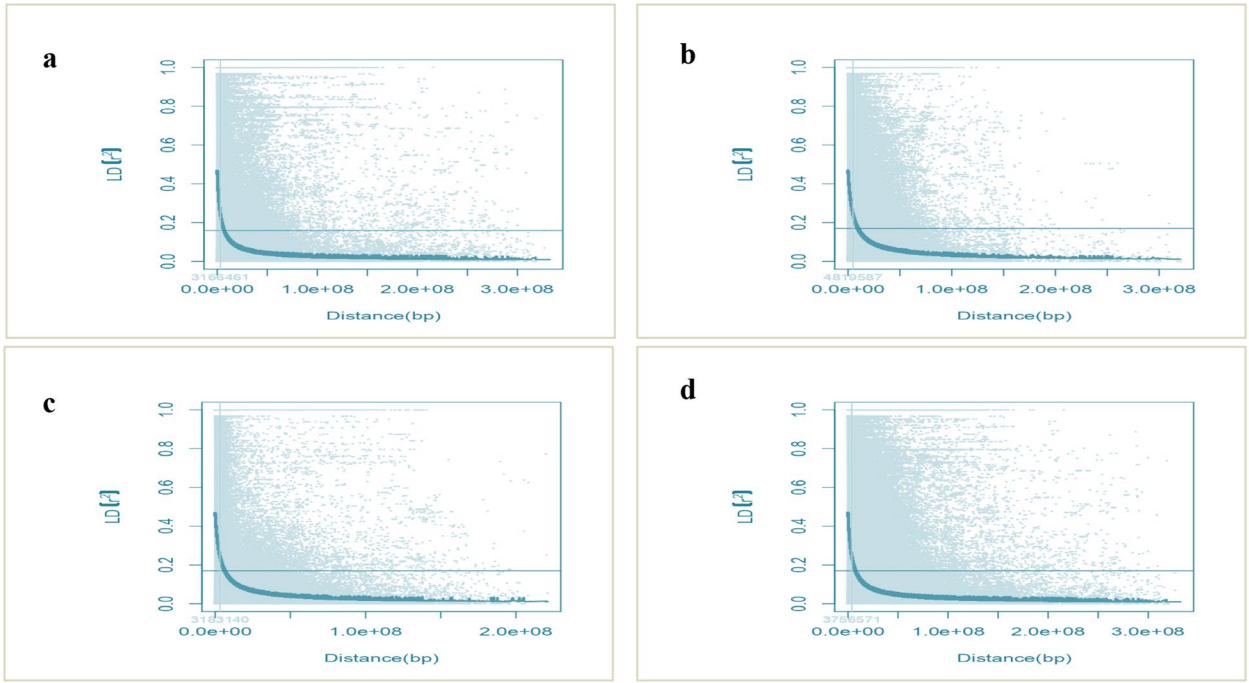

Fig. 3 LD decay plot with LOESS curve in red at $r^2 = 0.17$. **a** Sub-genome A, LD decay plot, **b** Sub-genome B LD decay plot, **c** Sub-genome D LD decay plot and (**d**) whole genome LD decay plot

Marker trait associations (MTAs)

A comprehensive MTA analysis using six different ML-GWAS models identified a total of 155 QTNs for twelve yield related traits, with a LOD score of ≥ 3 as the critical thresholds. These QTNs were selected based on consensus results from at least three ML-GWAS models. Among these, 42 QTNs, controlled by 20 SNPs were highly significant and consistent across multiple models (≥ 5) and environments (≥ 4). The proportion of phenotypic variation explained (PVE) by these SNPs ranged from 3–58% (Table 3), indicating that wheat yield parameters are influenced by several loci with varying effects, from small to moderate.

QTNs were identified in all twelve environments studied (Tables S7-a, b, c & d, S8-a, b, c & d, and S9-a, b, c & d). Specifically, five out of six ML-GWAS models found the following numbers of significant QTNs: FASTmrEMMA (35), mrMLM (173), FASTmrMLM (120), ISIS EM-BLASSO (28), and pLARmEB (77) (Fig. 4a). However, the pKWmEB model did not detect any QTN crossiing the significance threshold. The highest number of significant QTNs was observed for GYLD (18), followed by GERM_PCT (15), GC (15), DTHD (15), DTMT (15), MT_CT (13), GC_NDVI (12), DTFL (11), MT_NDVI (11), E_CG (10), DTB (10), TGW (10), AN_CT (10), GF_NDVI (9), PH (6), AN_NDVI (6), GF_CT (5), H_CT (4), and H_NDVI (3) (Fig. 4b). Chromosome 2D contained the most QTNs (29), followed by 2B (27), 3B (25), 1A (21), 2A (21), 6B (20), 1B (19), 7A (17), 7D (17), 5D (16), 4B (15), 5A (14), 3D (13), 4A (13), 5B (12), 6A (12), 3A (11), 1D (9), 6D (9), and 4D (7) (Fig. 4c). Manhattan plots showing robust QTNs identified by three or more ML-GWAS approaches for each trait are presented in Figs. 5a-s.

Most significant QTNs for grain yield and its component traits

QTNs for GYLD and DTB: Among the total identified QTNs for GYLD, QTN *qtn_nbpgr_GYLD_3B* (3B) holds the most promising position explaining the phenotypic variation of 9.84 – 19.89% (Table 3). It exhibited the highest LOD score ranging from 3.28 – 3.92 and was consistently identified across five GWAS models. Additionally, *qtn_nbpgr_GYLD_3B* was observed to be significant in at least four different environments. Nine significant QTNs for DTB viz., *qtn_nbpgr_DTB_1B* (Chr1B), *qtn_nbpgr_DTB_2B* (Chr2B), *qtn_nbpgr_DTB_7A* (Chr7A), *qtn_nbpgr_DTB_6B* (Chr6B), *qtn_nbpgr_DTB_6A* (Chr6A), *qtn_nbpgr_DTB_5A* (Chr5A), *qtn_nbpgr_DTB_1A.1* (Chr1A), *qtn_nbpgr_DTB_1A.2* (Chr1A) and *qtn_nbpgr_DTB_7D* (Chr7D), explained the variation in range of 3–39%. These QTNs were identified in at least four environments and in five out of six ML-GWAS methods (Table 3).

Table 3 Highly significant and consistent QTNs detected for various yield related traits in bread wheat

[a]Marker	Traits associated	QTN	CHR	Marker position (bp)	LOD score	'-log10(P)'	r2 (%)	[b]Detection method	No. of Environments
AX-95232570	DTB DTFL	*qtn_nbpgr_DTB_1B* *qtn_nbpgr_DTFL_1B*	1B	7479810	3.57–3.92	4.30—4.68	3.54 –7.09	1,2,3,4,5	5
AX-95226270	DTB DTFL DTHD MT_NDVI	*qtn_nbpgr_DTB_2B* *qtn_nbpgr_DTFL_2B* *qtn_nbpgr_DTHD_2B* *qtn_nbpgr_MTNDVI_2B*	2B	310933249	3.55—9.43	4.27–10.36	15.84—36.21	1,2,3,4,5	5
AX-95018072	DTB DTHD DTMT GF_NDVI MT_NDVI	*qtn_nbpgr_DTB_7A* *qtn_nbpgr_DTHD_7A* *qtn_nbpgr_DTMT_7A* *qtn_nbpgr_GFNDVI_7A* *qtn_nbpgr_MTNDVI_7A*	7A	22963445	3.24—4.17	3.95—4.93	9.02 – 18.98	1,2,3,4,5	4
AX-94946941	DTB DTFL DTHD DTMT	*qtn_nbpgr_DTB_6B* *qtn_nbpgr_DTFL_6B* *qtn_nbpgr_DTHD_6B* *qtn_nbpgr_DTMT_6B*	6B	50407384	3.44—10.19	4.16 –11.13	13.36 – 39.37	1,2,3,4,5	5
AX-94925147	DTB DTFL DTHD DTMT	*qtn_nbpgr_DTB_6A* *qtn_nbpgr_DTFL_6A* *qtn_nbpgr_DTHD_6A* *qtn_nbpgr_DTMT_6A*	6A	11555132	3.09—4.54	3.79 –5.32	16.05—36.04	1,2,3,4,5	7
AX-94876731	DTB DTFL DTHD	*qtn_nbpgr_DTB_5A* *qtn_nbpgr_DTFL_5A* *qtn_nbpgr_DTHD_5A*	5A	569452650	3.04—6.52	3.74—7.37	7.04—21.82	1,2,3,4,5	5
AX-94867479	DTB DTHD	*qtn_nbpgr_DTB_1A.1* *qtn_nbpgr_DTHD_1A.1*	1A	592099984	3.24—4.54	4.21—5.32	9.86 – 23.09	1,2,3,4,5	4
AX-94440483	DTB DTFL DTHD	*qtn_nbpgr_DTB_1A.2* *qtn_nbpgr_DTFL_1A* *qtn_nbpgr_DTHD_1A.2*	1A	532815438	3.51—3.55	8.24—4.28	3.45 – 7.53	1,2,3,4,5	8
AX-94436363	DTB DTFL DTHD DTMT	*qtn_nbpgr_DTB_7D* *qtn_nbpgr_DTFL_7D.1* *qtn_nbpgr_DTHD_7D* *qtn_nbpgr_DTMT_7D*	7D	165729745	3.29—6.96	4.00—7.82	3.01 – 14.15	1,2,3,4,5	5

Table 3 (continued)

[a]Marker	Traits associated	QTN	CHR	Marker position (bp)	LOD score	'-log10(P)'	r2 (%)	[b]Detection method	No. of Environments
AX-94468017	DTFL	*qtn_nbpg_ DTFL_7D.2*	7D	4026329	3.33—5.16	4.04—5.96	9.37 – 18.00	1,2,3,4,5	5
AX-94764856	DTHD	*qtn_nbpgr_ DTHD_6A*	6A	551836106	3.31—4.99	4.02—5.79	4.55 – 7.33	1,2,3,4,5	6
AX-94773648	DTMT	*qtn_nbpgr_ DTMT_4D*	4D	25987172	3.14—3.92	3.84—4.66	4.09 – 7.06	1,2,3,4,5	7
AX-95101968	E_GC	*qtn_nbpgr_ EGC_7D*	7D	295311788	10.64—15.69	12.23 –16.73	46.65 – 62.59	1,2,3,4,5	5
AX-94868586	G_PCT	*qtn_nbpgr_ GPCT_2D*	2D	293154747	3.88—6.79	4.63—7.65	14.79 – 40.12	1,2,3,4,5	5
AX-94543147	GYLD	*qtn_nbpgr_ GYLD_3B*	3B	819897421	3.28 – 3.92	3.78—4.06	9.84 – 19.89	1,2,3,4,5	5
AX-94601648	PH	*qtn_nbpgr_ PH_5A*	5A	637455248	3.01—5.73	3.71—6.56	4.37 – 10.37	1,2,3,4,5	7
AX-94622271	PH	*qtn_nbpgr_ PH_2A*	2A	725344929	3.43—5.15	4.15—5.95	12.95—21.96	1,2,3,4,5	4
AX-94817182	TGW	*qtn_nbpgr_ TGW_2B*	2B	58845605	3.42—4.82	4.14—5.61	15.48 –19.06 7	1,2,3,4,5	5
AX-94914663	TGW	*qtn_nbpgr_ TGW_1A*	1A	498807583	3.85—4.75	5.49—5.54	16.85—23.27	1,2,3,4,5	6
AX-94930926	TGW	*qtn_nbpgr_ TGW_4B*	4B	550256542	3.41—3.90	4.13—4.64	13.75 – 17.72	1,2,3,4,5	5

[a] Detected by 5 out of 6 ML-GWAS models and at ≥ 4 environments

[b] ML-GWAS methods (MrMLM-1, FASTMrMLM-2, FASTMrEMMA-3, pLARmEB-4, ISIS EM-BLASSO-5)

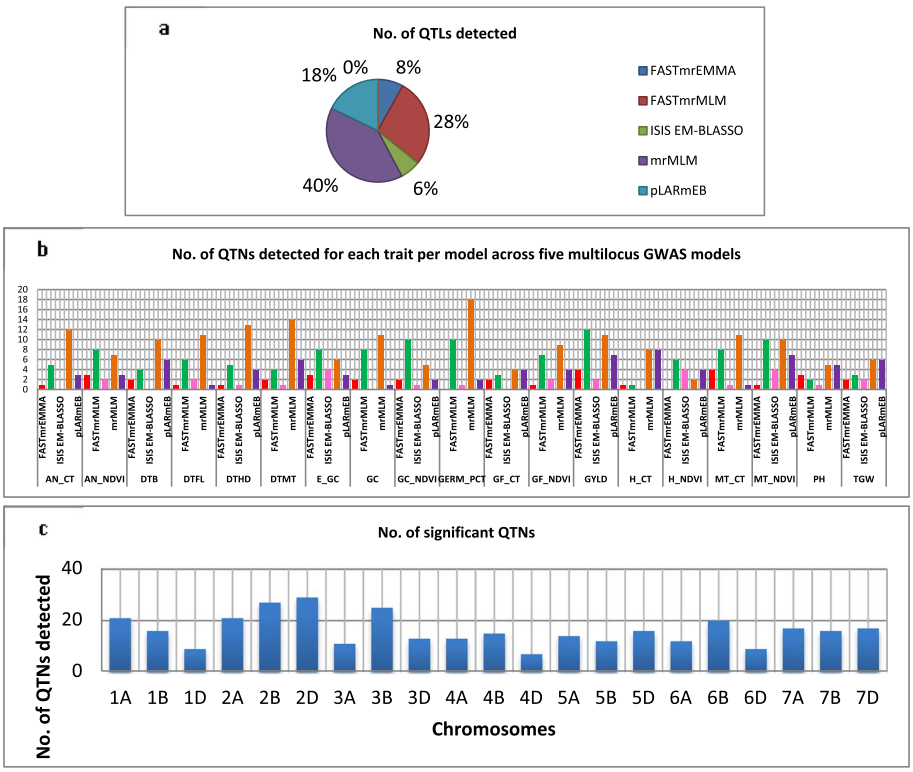

Fig. 4 Marker Trait Associations (**a**) Number of QTNs detected per ML-GWAS model, (**b**) No. of QTNs detected for each yield related trait per model across five multilocus GWAS models (**c**) Number of QTNs detected per chromosome for yield related traits (excluding pleiotropic QTNs)

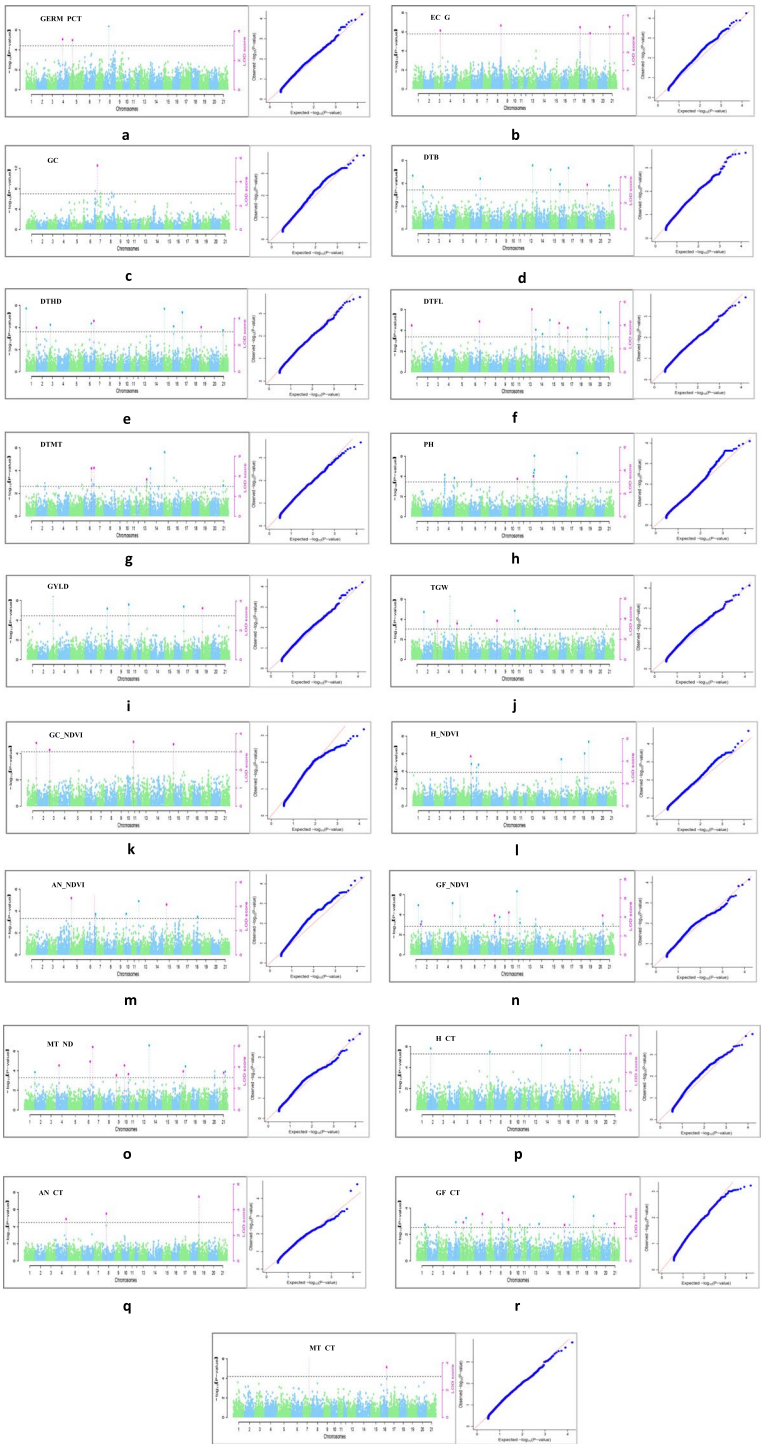

Fig. 5 Manhattan plot of significant QTNs (showing significant MTAs) for yield related traits with critical thresholds set at LOD score ≥ 3 (**a**) GERM_ PCT, (**b**) E_CG, (**b**) GC, (**d**) DTB (**e**) DTHD (**f**) DTFL, (**g**) DTMT, (**h**) PH, (**i**) GYLD (**j**) TGW, (**k**) GC_NDVI, (**l**) H_NDVI, (**m**) AN_NDVI, (**n**) GF_NDVI (**o**) MT_NDVI, (**p**) H_CT, (**q**) AN_CT, (**r**) GF_CT and (**s**) MT_CT

Two significant QTNs for PH, *qtn_nbpgr_PH_5A* (Chr5A) and *qtn_nbpgr_PH_2A* (Chr2A) were identified in at least four environments and by multiple models, explained 4.37 – 10.37% and 12.95—21.96% of total phenotypic variation, respectively (Table 3). For TGW, three significant QTNs, *qtn_nbpgr_TGW_2B* (Chr2B), *qtn_nbpgr_TGW_1A* (Chr1A) and *qtn_nbpgr_TGW_4B* (Chr4B), were identified in at least four environments and by five out of six ML-GWAS models, explaining proportions of total phenotypic variation in range of 15–23% (Table 3).

For DTFL, eight QTNs, *qtn_nbpgr_DTFL_1B* (Chr1B), *qtn_nbpgr_DTFL_2B (*Chr2B), *qtn_nbpgr_DTFL_6B* (Chr6B), *qtn_nbpgr_DTFL_6A* (Chr6A), qtn_*nbpgr_DTFL*_5A (Chr5A), *qtn_nbpgr_DTFL_1A* (Chr1A), *qtn_nbpgr_DTFL_7D.1* (Chr7D) and *qtn_nbpg_DTFL_7D.2* (Chr7D), were identified in at least four environments and by five out of six ML-GWAS models, explaining proportions of total phenotypic variation in the range of 3–39%. For DTHD, nine QTNs, *qtn_nbpgr_DTHD_2B* (Chr2B), *qtn_nbpgr_DTHD_7A* (Chr7A), *qtn_nbpgr_DTHD_6B* (Chr6B), *qtn_nbpgr_DTHD_6A* (Chr6A), *qtn_nbpgr_DTHD_5A* (Chr5A), *qtn_nbpgr_DTHD_1A.1* (Chr1A), *qtn_nbpgr_DTHD_1A.2* (Chr1A), *qtn_nbpgr_DTHD_7D* (Chr7D) and *qtn_nbpgr_DTHD_6A* (Chr6A) expressed the significant associations in multiple environments and GWAS models, explaining the phenotypic variation in range of 3–39%. Five significant QTNs on chromosomes 4D, 6B, 6A, 7D, 7A (*qtn_nbpgr_DTMT_7A*, *qtn_nbpgr_DTMT_6B*, *qtn_nbpgr_DTMT_6A*, *qtn_nbpgr_DTMT_7D* and *qtn_nbpgr_DTMT_4D*), was found to be associated with DTMT, explaining the PVE in range of 3–39% (Table 3).

The association *qtn_nbpgr_MTNDVI_2B* (Chr2B), *qtn_nbpgr_GFNDVI_7A* (Chr7A) and *qtn_nbpgr_MTNDVI_7A* (Chr7A) were significantly associated to NDVI. Moreover, the qtn_*nbpgr_EGC_7D* (Chr7D) and *qtn_nbpgr_GPCT_2D* (Chr2D) were significantly associated with E_CG and G_PCT, explaining the total PVE of 46.65 – 62.59% and 14.79 – 40.12% respectively. All these QTNs were detected in multiple environments and by five out of six ML-GWAS models which explains the reliability of these identified genomic regions for further analysis (Table 3).

Furthermore, to compare our findings with previous studies, a comprehensive chromosome map was constructed, integrating both the highly significant and consistent markers identified in this study and those reported in earlier research (Fig. 6). This approach provides a broader genomic perspective, facilitating the identification of overlapping regions and potential candidate genes associated with key traits.

Pleiotropic SNPs for more than one trait

In plants, the association of the same genomic region with multiple traits, known as pleiotropy, is quite common. In our study, we have identified a total of 9 SNPs associated with more than one yield related trait (Table 4). Among these, SNP AX-95018072 on chromosome 7A was linked to the highest number of traits (5), including DTB, DTHD, DTMT, GF_NDVI, and MT_NDVI. The markers AX-95226270 (Chr2B), AX-94436363 (Chr7D), AX-94925147 (Chr6A), and AX-94946941 (Chr6B) were each associated with four traits. Additionally, markers AX-94440483 (Chr1A) and AX-94876731 (Chr5A) were linked to three traits each, while AX-94867479 (Chr1A) and AX-95232570 (Chr1B) were associated with two traits each. Notably, chromosome 1A had the highest number of pleiotropic SNPs, with two such SNPs (Table 4).

Allelic effects of significant pleiotropic SNPs on respective phenotypes

On the basis of favorable allele analysis, three key pleiotropic SNPs (1A: AX-94867479; 5A: AX-94876731; and 7D: AX-94436363) were identified using three or more ML-GWAS methods to evaluate phenotypic variations across all traits (Fig. 7). It was found that each SNP had a significant effect on their corresponding traits ($p \leq 0.01$). The SNP AX-94867479 had a notable impact on DTB (qtn_nbpgr_DTB_1A) and DTHD (qtn_nbpgr_DTHD_1A). The SNP AX-94876731 influenced DTB (qtn_nbpgr_DTB_5A), DTFL (qtn_nbpgr_DTFL_5A), and DTHD (qtn_nbpgr_DTHD_5A). Similarly, the SNP AX-94436363 significantly affected DTB (qtn_nbpgr_DTB_7D), DTFL (qtn_nbpgr_DTFL_7D), DTHD (qtn_nbpgr_DTHD_7D), and DTMT (qtn_nbpgr_DTMT_7D). These associations highlight their possible role in managing multiple yield-related traits under heat stress in bread wheat.

Putative candidate gene identification and in-silico analysis

To identify potential candidate genes associated with the identified QTNs, we performed BLAST analysis against the IWGSC reference genome (IWGSC-refseq version 1.0) of *Triticum aestivum* (https://plants.ensembl.org/Triticum_aestivum/Tools/Blast) using the online resource Ensembl Plants. This analysis revealed candidate genes flanking the identified QTNs. To strengthen validation and enrich our results, we conducted an additional Gene Ontology (GO) annotation analysis using the DAVID online tool. This cross-validation approach confirmed our findings and provided deeper insights into the functional roles of the candidate genes (https://david.ncifcrf.gov/summary.jsp) (Table S10). Most of the SNPs were located near transcripts coding for

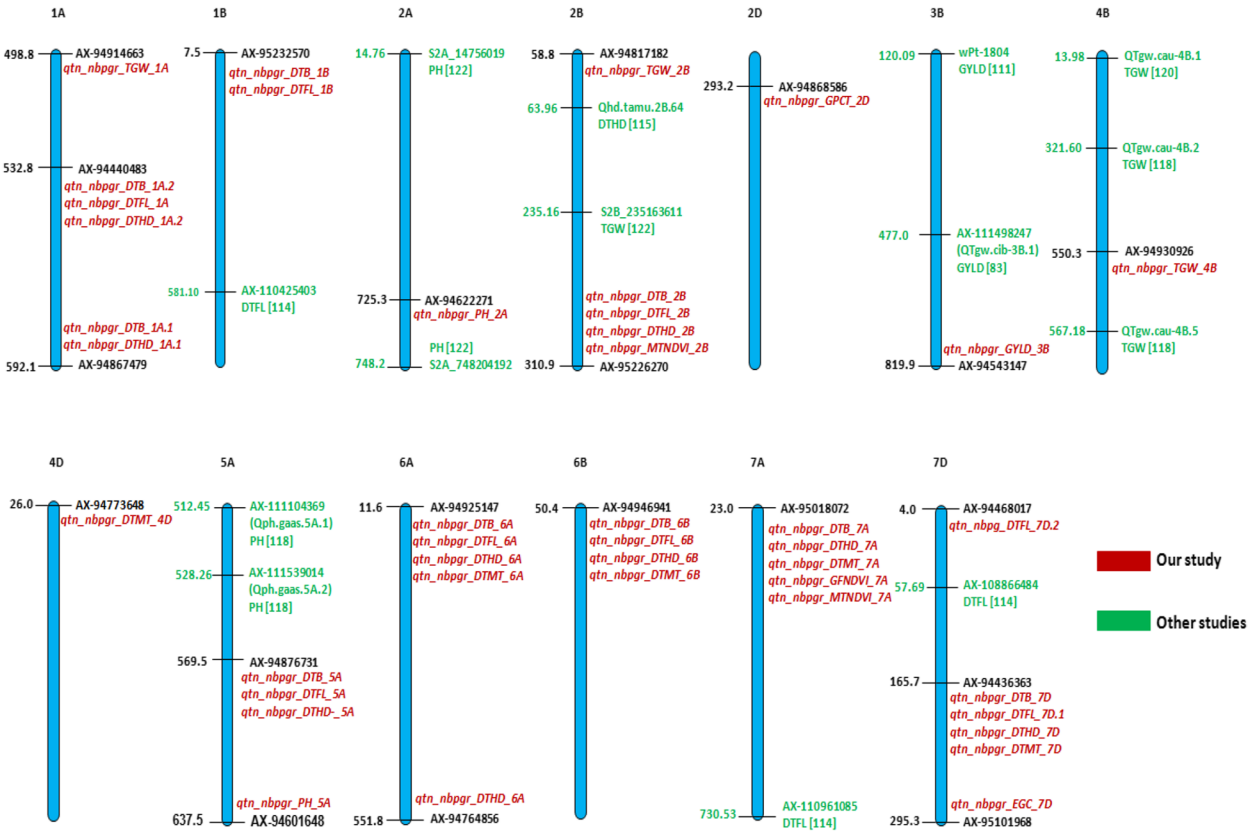

Fig. 6 Comprehensive chromosome map, integrating both the highly significant and consistent markers identified in this study and those reported in earlier research. Red color indicates our study; green color indicates previous studies

various proteins or transcription factors, except for SNPs AX-95232570 and AX-946016. The SNPs were located near genes coding for various proteins, including Chaperonin Cpn60/GroEL/TCP-1 family, Glycosyl hydrolase, five-bladed beta-propellor domain superfamily, Chloroplast envelope membrane protein (CemA), GTP cyclohydrolase 1, Target SNARE coiled-coil homology domain, Papain-like cysteine peptidase superfamily, SNW/SKI-interacting protein, Signal transduction response regulator (receiver domain), and KRR1 interacting protein 1, among others (Table 5). SNP AX-94876731 was found in a protein-coding region where the protein is still unknown. Among the eighteen identified genes, *TraesCS7D02G208200, TraesCS1A02G346200, TraesCS1A02G444100, TraesCS5A02G369100, TraesCS6A02G023100, TraesCS6B02G073900, TraesCS7A02G049300,* and *TraesCS2B02G257800* were pleiotropic, supposed to be associated with multiple traits (Table 5).

Validation of QTNs through KASP marker approach

KASP primers (Table S11) have been designed from 51 QTNs of which 33 found to be polymorphic on panel of 101 lines consisting of heat stress tolerant and susceptible lines (Tables S12a & b). We prioritized QTNs that were consistently identified by at least three ML-GWAS models used in our study and demonstrated high statistical significance (low *p*-values and high r^2 values) across multiple environments. The panel has been procured from BISA, Ludhiana. The validation set was partitioned into two categories (Tolerant and Susceptible). Among the 101 genotypes, 66 were classified as Tolerant (0–49%), while 35 genotypes were identified as Susceptible (29–76%). The three pivotal KASP markers, denoted as *AX-95018072* (associated with DTB, DTHD, DTMT, GF_NDVI, and MT_NDVI), *AX-94946941* (associated with DTB, DTFL, DTHD and DTMT) and *AX-95232570* (associated with DTB and DTFL) were found to be associated with respective QTNs in this panel (Table 6). These markers, situated on distinct chromosomal locations, namely 7A, 6B and 1B respectively, manifested remarkable statistical significance in the context of QTNs concerning heat stress. Notably, the alternative alleles of these markers exerted discernible and substantial impacts on the phenomenon of heat stress, signifying tolerance.

Table 4 Pleiotropic SNPs associated with multiple yield related traits

Marker	Traits associated	QTN	CHR	Marker position (bp)	LOD score	'-log10(P)'	r2 (%)
AX-95232570	DTB DTFL	*qtn_nbpgr_DTB_1B* *qtn_nbpgr_DTFL_1B*	1B	7479810	3.57–3.92	4.30—4.68	3.54 –7.09
AX-95226270	DTB DTFL DTHD MT_NDVI	*qtn_nbpgr_DTB_2B* *qtn_nbpgr_DTFL_2B* *qtn_nbpgr_DTHD_2B* *qtn_nbpgr_MTNDVI_2B*	2B	310933249	3.55—9.43	4.27–10.36	15.84—36.21
AX-95018072	DTB DTHD DTMT GF_NDVI MT_NDVI	*qtn_nbpgr_DTB_7A* *qtn_nbpgr_DTHD_7A* *qtn_nbpgr_DTMT_7A* *qtn_nbpgr_GFNDVI_7A* *qtn_nbpgr_MTNDVI_7A*	7A	22963445	3.24—4.17	3.95—4.93	9.02 – 18.98
AX-94946941	DTB DTFL DTHD DTMT	*qtn_nbpgr_DTB_6B* *qtn_nbpgr_DTFL_6B* *qtn_nbpgr_DTHD_6B* *qtn_nbpgr_DTMT_6B*	6B	50407384	3.44—10.19	4.16 –11.13	13.36 – 39.37
AX-94925147	DTB DTFL DTHD DTMT	*qtn_nbpgr_DTB_6A* *qtn_nbpgr_DTFL_6A* *qtn_nbpgr_DTHD_6A* *qtn_nbpgr_DTMT_6A*	6A	11555132	3.09—4.54	3.79 –5.32	16.05—36.04
AX-94876731	DTB DTFL DTHD	*qtn_nbpgr_DTB_5A* *qtn_nbpgr_DTFL_5A* *qtn_nbpgr_DTHD_5A*	5A	569452650	3.04—6.52	3.74—7.37	7.04—21.82
AX-94867479	DTB DTHD	*qtn_nbpgr_DTB_1A* *qtn_nbpgr_DTHD_1A*	1A	592099984	3.24—4.54	4.21—5.32	9.86 – 23.09
AX-94440483	DTB DTFL DTHD	*qtn_nbpgr_DTB_1A* *qtn_nbpgr_DTFL_1A* *qtn_nbpgr_DTHD_1A*	1A	532815438	3.51—3.55	8.24—4.28	3.45 – 7.53
AX-94436363	DTB DTFL DTHD DTMT	*qtn_nbpgr_DTB_7D* *qtn_nbpgr_DTFL_7D* *qtn_nbpgr_DTHD_7D* *qtn_nbpgr_DTMT_7D*	7D	165729745	3.29—6.96	4.00—7.82	3.01 – 14.15

In the subsequent validation phase, the study meticulously identified specific allelic variants correlated with the attributes of heat tolerance. Moreover, allelic variant G of markers AX-95018072, AX-94946941 and AX-95232570 exhibiting a statistical significance (p-value < 0.001), emerged prominently associated with heat stress tolerance (Fig. 8).

Discussion

Wheat is one of the most important staple food crops worldwide, providing a significant segment of the daily calories and protein for billions of people [1, 86]. However, wheat production is increasingly challenged by various abiotic stresses, among which heat stress is a major constraint, especially in the context of global climate change [3, 87, 88]. Heat stress adversely affects wheat growth and yield, particularly when it occurs during the reproductive and grain-filling stages [2, 89]. Therefore, developing heat-tolerant wheat varieties is crucial for sustaining wheat productivity and ensuring food security in the face of changing climatic conditions. This analysis aimed to map QTNs and identify SNP markers linked to agronomic traits in timely and late-sown wheat to expedite marker-assisted selection (MAS) for developing heat-tolerant wheat varieties.

Wheat germplasm collections from various geographical regions provide a rich source of genes, alleles, and QTNs that contribute to heat stress tolerance [20, 90]. With the advent of high-throughput genotyping [25, 91], phenotyping [26], advanced bioinformatics tools and packages [27], studying these germplasm collections has become more feasible, enabling the effective use of their genetic diversity [92, 93]. A current study on a diverse AM panel of 126 wheat genotypes, showed significant phenotypic variation for the yield traits evaluated under normal and heat stress conditions across twelve environments. This indicates the suitability of this panel for AM of heat tolerance traits in wheat. Similar results on the presence of significant phenotypic variation in AM panels of wheat have been reported in previous studies [33, 94]. The AM panel tested across twelve different environments identified key heat-tolerant QTNs that can be used to broaden the genetic base for heat stress tolerance in bread wheat. AM has emerged as a powerful tool for dissecting complex traits and identifying trait-associated QTLs/genes in many crop species including wheat [28, 31–33]. The

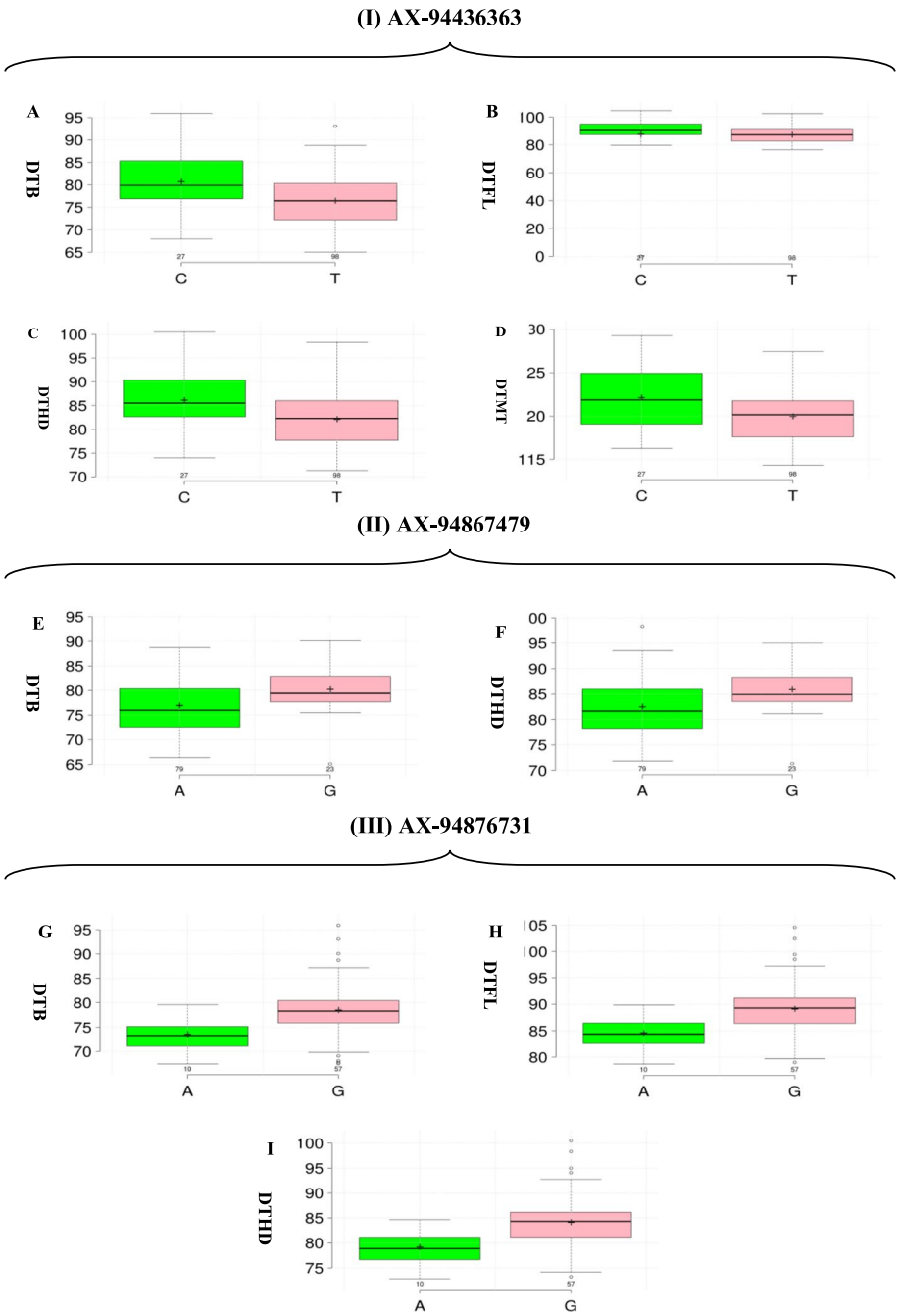

Fig.7 Boxplots depicting the significant effects ($p < 0.01$) of three key pleiotropic SNPs on their corresponding traits, with germplasm lines grouped by superior and inferior allele types. The x-axis shows the two alleles for each QTN, while the y-axis represents the phenotypic values. Figure 6(I) illustrates SNP AX-94436363, with subfigures (**A**–**D**) showing allelic differences for DTB, DTFL, DTHD, and DTMT, where the superior alleles for QTNs qtn_nbpgr_DTB_7D, qtn_nbpgr_DTFL_7D, qtn_nbpgr_DTHD_7D, and qtn_nbpgr_DTMT_7D were all C. Figure 6(II) displays SNP AX-94867479, with subfigures (**E**–**F**) showing allelic differences for DTB and DTHD, with the superior alleles for QTNs qtn_nbpgr_DTB_1A and qtn_nbpgr_DTHD_1A being G. Figure 6(III) shows SNP AX-94876731, with subfigures (**G**–**I**) representing allelic differences for DTB, DTFL, and DTHD, where the superior alleles for QTNs qtn_nbpgr_DTB_5A, qtn_nbpgr_DTFL_5A, and qtn_nbpgr_DTHD_5A were also G

yield-related traits investigated included GERM_PCT, E_CG, GC, DTB, DTHD, DTFL, DTMT, PH, GYLD, TGW, NDVI, and canopy temperature (CT).

GERM_PCT and E_CG are important traits for crop establishment, which can influence the final yield [95, 96]. GC is associated with early vigor and can affect the

Table 5 Putative candidate genes Linked to significant SNPs along with their molecular functions

SNP	Trait	Position (bp)	Gene	Description/ annotation	Function	References
AX-94436363	DTB, DTFL, DTHD, DTMT	7D: 165727668–165735752	TraesCS7D02G208200	Chaperonin Cpn60/GroEL/TCP-1 family	protein folding, trafficking and disaggregation under stressful conditions	[69]
AX-94440483	DTB, DTFL, DTHD	1A:532814880–532821932	TraesCS1A02G346200	Pyruvate phosphate dikinase, AMP/ATP-binding	CO_2 Assimilation, Abiotic Stress Tolerance in C3 Plants Under Elevated CO2 Conditions	[70]
AX-94867479	DTB, DTHD	1A:592099464–592101364	TraesCS1A02G444100	Signal transduction response regulator, receiver domain	enhancement of plant stress tolerance	[71]
AX-94876731	DTB, DTFL, DTHD	5A:569452203–569456729	TraesCS5A02G369100	Uncharacterized protein	–	–
AX-94925147	DTB, DTFL, DTHD, DTMT	6A:11554651–11558118	TraesCS6A02G023100	Glycosyl hydrolase, five-bladed beta-propellor domain superfamily	activation of phytohormones, cell wall remodeling, lignification, and response to biotic and abiotic stresses	[72]
AX-94946941	DTB, DTFL, DTHD, DTMT	6B:50407053–50411048	TraesCS6B02G073900	Papain-like cysteine peptidase superfamily	Plant abiotic stress response, contribute to processes such as germination, development, senescence, and immunity	[73]
AX-95018072	DTB, DTHD, DTMT, GF_NDVI, MT_NDVI	7A:22961615–22964184	TraesCS7A02G049300	Target SNARE coiled-coil homology domain	endosomal trafficking, transports cargos that include storage proteins, reactive oxygen species (ROS), and unidentified substances, facilitating responses to abiotic stresses, pivotal role in cytokinesis and the initiation of innate immune responses under adverse environments	[74]
AX-95226270	DTB, DTFL, DTHD, MT_NDVI	2B:310928737–310944356	TraesCS2B02G257800	Pyruvate kinase	energy metabolism, glycolysis	[75]
AX-94468017	DTFL	7D:4025269–4028988	TraesCS7D02G008500	NAC domain superfamily	regulates flowering, leaf senescence, root development, cell division, secondary cell wall biosynthesis,, seed development, grain yield and quality under heat and drought stress	[76]
AX-94764856	DTHD	6A:551834610–551837285	TraesCS6A02G315200	SNW/SKI-interacting protein	influences endoreduplication and cell growth	[77]
AX-94773648	DTMT	4D:25986916–25991603	TraesCS4D02G050200	Leucine-rich repeat-containing N-terminal, plant-type	plant immune response	[78]
AX-95101968	E_GC	7D:295311643–295322727	TraesCS7D02G283700	Chloroplast envelope membrane protein, CemA	Involved in The Male-Sterility of K-Type CMS	[79]
AX-94868586	GERM_PCT	2D:293146585–293155918	TraesCS2D02G248600	Proline-tRNA, ligase, chloroplastic/mitochondrial	imparts stress tolerance by maintaining cell turgor or osmotic balance under stressful environments	[80]
AX-94543147	GYLD	3B:819896362–819902003	TraesCS3B02G597800	Peptidase C13, legumain	germination	[81]
AX-94622271	PH	2A:725343348–725347869	TraesCS2A02G492900	GTP cyclohydrolase 1	synthesizing the folate precursors pterin	[82]

Table 5 (continued)

SNP	Trait	Position (bp)	Gene	Description/ annotation	Function	References
AX-94817182	TGW	2B:58843544–58846856	TraesCS2B02G099500	Fatty acid desaturase domain	response to environmental stresses	[83]
AX-94914663	TGW	1A:498806535–498809142	TraesCS1A02G307300	KRR1 interacting protein 1	Ribosomal biosynthesis	[84]
AX-94930926	TGW	5B:550255360–550257476	TraesCS5B02G372000	Manganese-dependent ADP-ribose/ CDP-alcohol diphosphatase	glycerophospholipid metabolism pathway	[85]

Table 6 Novelty and utility of KASP validated markers

KASP Marker	Associated Gene/Protein	Novelty	Utility
AX-94946941	Gene: TraesCS6B02G073900 Protein: Papain-like cysteine peptidase (PLCP) superfamily member	First association with DTB, DTFL, DTHD, DTMT in bread wheat. Located on chromosome 6B	Enhances wheat resilience to stress, improving yield
AX-95018072	Gene: TraesC-S7A02G049300 Protein: Contains Target SNARE coiled-coil homology domain	First link to DTB, DTHD, DTMT, GF_NDVI, MT_NDVI in bread wheat. On chromosome 7A	Aids stress response, maintains homeostasis. Potential for breeding heat-tolerant wheat
AX-95232570	Gene: Unknown Protein: Unknown	First association with DTB, DTFL in bread wheat. Located on chromosome 1B	Validated marker. Potential for developing heat-tolerant wheat varieties

crop's ability to suppress weeds and conserve soil moisture [97, 98]. Days to booting, heading, flowering, and maturity are important phenological traits that determine the duration of different developmental stages and can affect the crop's adaptation to various environments [99–101]. PH is an important agronomic trait that can influence lodging resistance, harvest index, and final yield [102, 103]. GYLD is the most important trait for wheat improvement, while TGW is a key component of grain yield [104, 105]. NDVI is a widely used vegetation index that can reflect the crop's biomass, vigor, and photosynthetic capacity [106, 107]. CT is an indicator of the crop's transpiration efficiency and has been used as a selection criterion for heat and drought tolerance in wheat [108].

The yield related traits exhibited significant differences between normal and heat stress regimes, with traits like GERM_PCT, GC, DTB, DTHD, DTFL, DTMT, PH, GYLD, and TGW showed the reduced performance while performance of E_GC, H_CT, AN_CT, GF_CT and MT_CT were enhanced under heat stress. Heat stress is known to adversely affect wheat growth and yield traits. Further, high temperatures, especially during reproductive stages, can lead to reduced grain number, grain weight and final yield [2, 3, 109, 110]. Our results are in agreement with these previous studies demonstrating the negative impacts of heat stress on wheat. Additionally, heritability was calculated on a line-mean basis using the method described by Gilmour et al. (1995) [62].

The GGE biplot analysis is a powerful tool for visualizing genotype by environment interactions and identifying stable and high-performing genotypes across different environments [61]. Trait-wise GGE biplot analysis was performed to identify the best-performing genotypes and assess their stability across the twelve environments for yield component traits, including GERM_PCT, E_CG, GC, DTB, DTHD, DTMT, PH, TGW, and GYLD. In our study, several genotypes were identified as the best performers for specific traits across all environments. For example, genotypes EC464070 and EC576792 were the best performers for GERM_PCT, while IC279335 and IC252668 were the most promising for GYLD across all locations. Furthermore, the mean vs. stability analysis revealed that some genotypes, such as IC138589, IC138600, and IC138637 for GERM_PCT, and IC393128 and IC252469 for GYLD, exhibited high stability and above-average performance. Identifying genotypes with both high performance and stability is important for developing varieties that can perform well under diverse environmental conditions [60].These findings are consistent with previous studies that have used GGE biplot analysis to identify stable and high-performing genotypes for various traits in wheat [111, 112].

In GWAS, population structure can be a confounding factor that needs to be addressed to prevent false associations. Two popular methods for inferring population structure in a genome-wide association panel using high-density SNPs are STRUCTURE and kinship analysis [64, 65]. The analysis of population structure in the current genotypic panel revealed the existence of two distinct sub-populations, designated as SP1 and SP2, consisting of 61 and 65 lines, respectively. Additionally, the relationships among the genotypes were investigated using phylogenetic tree analysis to gain further insights into their genetic relatedness and evolutionary history. Similar studies have been conducted in various crop species, such as oats [113], potato [114], rice [115], maize [116], wheat [117], Arabidopsis [118] and foxtail millet [119], highlighting the importance of population structure in GWAS to minimize false-positive associations and to identify genetic loci associated with agronomic traits of interest.

LD plays a significant role in determining the effectiveness of marker trait association analysis [120]. When LD is high, it means that a smaller number of markers are needed to adequately cover the entire genome compared to situations where LD is low [121].

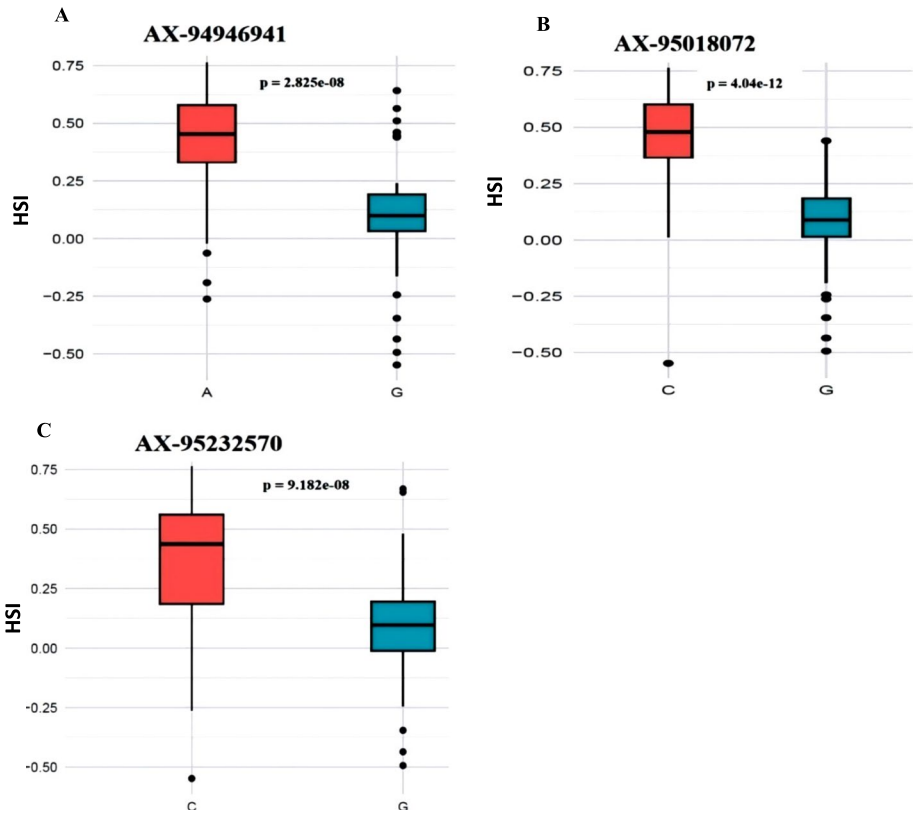

Fig. 8 Kruskal–Wallis test confirms significant Heat Susceptibility Index (HSI) differences between alleles of three KASP validated markers (**A**) AX-94946941, (**B**) AX-95018072 and (**C**) AX-95232570

This information is valuable in deciding the appropriate quantity of loci required for conducting a comprehensive whole-genome scan. In essence, understanding the level of LD in a population helps researchers optimize the number of markers necessary for their studies, ultimately saving time and resources while ensuring sufficient coverage of the genome [120]. In outcrossing crop species like maize, LD blocks are observed at shorter distances, leading to faster decay. In contrast, self-pollinated crops exhibit longer LD blocks with slower decay rates, as seen in wheat [31, 122]. In this study, the presence of population structure in the selected wheat germplasm led to higher LD values due to admixtures within both subpopulations. As a result, many distinct loci exhibited significant LD. The rate of LD decay varied among the sub-genomes, with the A sub-genome showing the fastest decay, followed by the D and B sub-genomes, respectively. The more rapid decay of LD in the A sub-genome of wheat can be attributed to a combination of factors, including recombination rates, population history, and gene flow. These findings are consistent with the results reported in previous studies conducted by [45, 123–125].

AM has emerged as a powerful tool for dissecting complex traits and identifying trait-associated QTLs/genes in many crop species [28, 29, 31, 32]. ML-GWAS are considered more advanced and effective than SL-GWAS for identifying genetic markers associated with complex traits. Recent studies by [126, 127], and [45] have highlighted the superiority of ML-GWAS methods for mapping complex traits. In the present study, a total of six ML-GWAS models were employed to investigate the association between genetic markers and the target trait. These models include mrMLM, FASTmrMLM, FASTmrEMMA, pLARmEB, ISIS EM-BLASSO, and pKWmEB, which have been previously described and utilized in various studies [38, 39, 41, 42, 45]. However, the pKWmEB model did not detect any QTNs above the significance threshold. By applying these diverse ML-GWAS approaches, the researchers aimed to identify the most significant markers linked to the trait of interest, providing a robust and comprehensive analysis of the genetic basis of the complex trait under investigation.

A total of 155 significant QTNs for the 12 yield-related traits, with 42 highly significant and consistent QTNs, regulated by 20 SNPs, were detected by five out of six multi-locus GWAS models and in multiple environments

at LOD score ≥ 3. The R^2 values of the QTNs ranged from 3 to 58%, indicating a significant range of phenotypic variation observed for these parameters. These QTNs provide valuable insights into the genetic architecture of heat tolerance in wheat and can be useful for marker-assisted breeding. One of the major QTN for GYLD was located on chromosome 3B (*qtn_nbpgr_GYLD_3B*), which is consistent with previous reports of major yield QTLs on this chromosome [105, 128, 129] (Fig. 6). Notably, the yield QTL on 3B identified by Bennett et al. (2012) [129], was also found to be associated with CT, in agreement with our findings. This suggests that this region on 3B may harbor important genes for heat tolerance that can influence multiple yield-related traits. Several significant QTNs for phenological traits such as DTB, DTFL, and DTHD on chromosomes 1B, 2B, 6A, 6B, 7A, and 7D were also identified in this study. Previous studies have reported QTLs for heading date and flowering time on these chromosomes in wheat as well [130–132] (Fig. 6). Some of these QTLs, such as those on 2B and 7A, have been found to be stable across multiple environments [130, 132], which is consistent with our findings. For PH, we identified significant QTNs on chromosomes 5A (*qtn_nbpgr_PH_*5A) and 2A (*qtn_nbpgr_PH_2A*). PH is known to be controlled by major genes such as *Rht-B1* and *Rht-D1* located on chromosomes 4B and 4D, respectively [133]. However, several other QTLs for PH have been reported on various chromosomes, including 5A and 2A [134–136] (Fig. 6). These additional QTLs may represent genes that modulate PH in a more subtle manner and could be useful for fine-tuning PH to optimize yield potential. TGW is an important yield component that is often affected by HS [3, 137]. We have identified significant QTNs for TGW on chromosomes 2B (*qtn_nbpgr_TGW_2B*), 1A (*qtn_nbpgr_TGW_1A*), and 4B (*qtn_nbpgr_TGW_4B*). QTNs for TGW have also been previously reported on these chromosomes in wheat [138, 139]. Notably, a major QTL for TGW on chromosome 2B was recently identified by Jamil et al. (2018) [136], which explained up to 20% of the phenotypic variation (Fig. 6). This QTL maps close to the QTN (*qtn_nbpgr_TGW_2B*) identified in our study, suggesting that they may represent the same gene or genes.

In addition to these major QTNs, we also identified several multi-trait SNPs that were associated with multiple yield-related traits. Multi-trait SNPs are indicative of pleiotropic genes or closely linked genes that can simultaneously influence multiple traits. Such multi-trait loci are highly valuable for breeding as they can potentially enable the simultaneous improvement of several desirable traits. In our study, a notable multi-trait QTN was identified on chromosome 7A, which was associated with five traits—DTB, DTHD, DTMT, GF NDVI, and MT NDVI. This QTN may represent a key locus for heat tolerance that can influence both phenological and physiological traits related to yield under HS.

Putative candidate gene identification and in-silico analysis are important steps in understanding the biological mechanisms underlying the detected MTAs [31, 140]. In our study, we have identified 18 putative candidate genes in close proximity to the significant SNPs associated with the yield-related traits under heat stress (Table 5). These candidate genes encoded proteins involved in various biological processes, such as stress response, signaling, and protein folding. In-silico analysis of these candidate genes using tools like Ensemble Plants, BLAST etc., provided insights into their potential functions and roles in HS response. The identification of candidate genes and their functional characterization is important for developing functional markers and targeted breeding strategies for heat tolerance in wheat [31, 140].

The validation of the identified QTNs is a critical step in confirming their usefulness for MAS. Three major SNPs, *AX-95018072* (associated with DTB, DTHD, DTMT, GF_NDVI, and MT_NDVI), *AX-94946941* (associated with DTB, DTFL, DTHD, and DTMT), and *AX-95232570* (associated with DTB and DTFL), were successfully validated using KASP markers in an independent panel of heat-tolerant and susceptible wheat lines. Previous studies have also used KASP markers for the successful validation of QTLs and MAS in wheat. For example, Rasheed et al. (2016) [50] developed and validated KASP markers for key genes associated with grain yield, quality, and disease resistance traits in wheat. Similarly, Kumar et al., (2022) [56] and Pradhan et al., (2023) [57] used KASP markers to validate QTLs for various traits in wheat, demonstrating their potential for marker-assisted breeding.

Conclusion

In conclusion, our study successfully identified novel QTNs and candidate genes associated with heat tolerance and yield-related traits in wheat through a comprehensive GWAS approach. The QTNs identified not only aligned with previously reported QTLs and genes for yield-related traits but also revealed several novel loci, expanding the current genetic knowledge. The validated KASP markers can now serve as valuable tools in marker-assisted breeding programs aimed at developing heat-tolerant wheat varieties. These findings significantly enhance our understanding of the genetic basis of heat tolerance in wheat, offering practical resources for breeders to accelerate the development of heat-resilient varieties. In light of increasing global temperatures and unpredictable climate patterns, such advancements are

crucial for safeguarding wheat production and ensuring food security in the face of climate change. Our research contributes to long-term strategies to breed crops that can withstand environmental stresses, thus supporting sustainable agriculture.

Supplementary Information

The online version contains supplementary material available at https://doi.org/10.1186/s12870-025-06285-4.

Supplementary Material 1.

Supplementary Material 2.

Acknowledgements
We are thankful to Director ICAR-NBPGR, New Delhi, for providing funding and technical assistance to our study. We are also thankful to Dr. Uttam Kumar, and Mr Manish for their support in field trials at different locations.

Authors' contributions
LB and SK gave concept and methodology. LB, AK, NB and DS analyzed the data. LB, AM, MH and NB wrote the aminj manuscript. SK, GP gave funding acquisition. SK, RB, DC, SK managed resources for the experiment. All authors reviewed the manuscript.

Funding
Financial assistance from ICAR- National Bureau of Plant Genetic Resources through ICAR, CABin project India "Germplasm characterization and trait discovery in wheat using genomic approaches and its Integration for improving climate resilience, productivity and nutritional quality" under mission programme of "Characterization of Genetic Resources" (Project code-1006445).

Data availability
Data is provided within the manuscript and supplementary information files.

Declarations

Ethics approval and consent to participate
Not applicable.

Consent for publication
Not applicable.

Competing interests
The authors declare no competing interests.

Author details
[1]ICAR-National Bureau of Plant Genetic Resources, Pusa Campus, New Delhi, 110012, India. [2]ICAR- Indian Agricultural Statistics Research Institute, New Delhi, India. [3]School of Plant, Environmental and Soil Science, LSU AgCenter, Louisiana State University, Baton Rouge, USA. [4]ICAR- Indian Agricultural Research Institute, New Delhi, India. [5]Punjab Agricultural University, Ludhiana, India. [6]Borlaug Institute for South Asia (BISA, CIMMYT-India, BISA Farm Ladhowal, Ludhiana, Punjab 141008, India.

Received: 24 November 2024 Accepted: 20 February 2025
Published online: 01 March 2025

References

1. Shiferaw, B., Smale, M., Braun, H., Duveiller, E., Reynolds, M., & Muricho, G. (2013). Crops that feed the world 10. Past successes and future challenges to the role played by wheat in global food security. Food Security, 5(3), 291–317. https://doi.org/10.1007/s12571-013-0263-y.
2. Farooq M, Bramley H, Palta JA, Siddique KH. Heat stress in wheat during reproductive and grain-filling phases. Crit Rev Plant Sci. 2011;30:491–507. https://doi.org/10.1080/07352689.2011.615687.
3. Farhad, M., Kumar, U., Tomar, V., Bhati, P. K., J, N. K., Kishowar-E-Mustarin, N., Barek, V., Brestic, M., & Hossain, A. Heat stress in wheat: a global challenge to feed billions in the current era of the changing climate. Frontiers in Sustainable Food Systems, 7 (2023). https://doi.org/10.3389/fsufs.2023.1203721.
4. Lobell DB, Schlenker W, Costa-Roberts J. Climate trends and global crop production since 1980. Science. 2011;333:616–20. https://doi.org/10.1126/science.1204531.
5. Asseng, S., Ewert, F., Martres, P., Rotter, R. P., Lobell, D. B., Cammarano, D., Kimball, B. A., Ottman, M. J., Wall, G. W., White, J. W., Reynolds, M. P., Alderman, P. D., Prasad, P. V. V., Aggarwal, P. K., Anothai, J., Basso, B., Biernath, C., Challinor, A. J., De Sanctis, G., . . . Zhu, Y. Rising temperatures reduce global wheat production. Nature Climate Change, 5 (2014) 143–147. https://doi.org/10.1038/nclimate2470.
6. Gupta AK, Agrawal M, Yadav A, Yadav H, Mishra G, Gupta R, Singh A, Singh J, Singh P. The effect of climate change on wheat production: Present patterns and upcoming difficulties. International Journal of Environment and Climate Change. 2023;13:4408–17. https://doi.org/10.9734/ijecc/2023/v13i113621.
7. Sun H, Wang Y, Wang L. Impact of climate change on wheat production in China. Eur J Agron. 2024;153: 127066. https://doi.org/10.1016/j.eja.2023.127066.
8. Nahar, K., Ahamed, K. U., & Fujita, M. Phenological Variation and its Relation with Yield in several Wheat (Triticum aestivum L.) Cultivars under Normal and Late Sowing Mediated Heat Stress Condition. Notulae Scientia Biologicae, 2 (2010) 51–56. https://doi.org/10.15835/nsb234723.
9. Akter, N., & Islam, M. R. Heat stress effects and management in wheat. A review. Agronomy for Sustainable Development, 37 (2017). https://doi.org/10.1007/s13593-017-0443-9.
10. Sarkar S, Islam A, Barma N, Ahmed J. Tolerance mechanisms for breeding wheat against heat stress: A review. S Afr J Bot. 2021;138:262–77. https://doi.org/10.1016/j.sajb.2021.01.003.
11. Sareen S, Budhlakoti N, Mishra KK, Bharad S, Potdukhe NR, Tyagi BS, Singh GP. Resilience to terminal drought, heat, and their combination stress in wheat genotypes. Agronomy. 2023;13:891. https://doi.org/10.3390/agronomy13030891.
12. Djanaguiraman, M., Narayanan, S., Erdayani, E., & Prasad, P. V. V. Effects of high temperature stress during anthesis and grain filling periods on photosynthesis, lipids and grain yield in wheat. BMC Plant Biology, 20 (2020). https://doi.org/10.1186/s12870-020-02479-0.
13. Dubey, R., Pathak, H., Chakrabarti, B., Singh, S., Gupta, D. K., & Harit, R Impact of terminal heat stress on wheat yield in India and options for adaptation. Agricultural Systems, 181 (2020) 102826. https://doi.org/10.1016/j.agsy.2020.102826.
14. Khan, I., Wu, J., & Sajjad, M. Pollen viability-based heat susceptibility index (HSIpv): A useful selection criterion for heat-tolerant genotypes in wheat. Frontiers in Plant Science, 13 (2022). https://doi.org/10.3389/fpls.2022.1064569.
15. Hafeez MB, Zahra N, Kausar A, Li J, Rehman A, Farooq M. Influence of heat stress during grain development on the wheat grain yield, quality, and composition. J Soil Sci Plant Nutr. 2023. https://doi.org/10.1007/s42729-023-01386-1.
16. Cossani CM, Reynolds MP. Physiological traits for improving heat tolerance in wheat. Plant Physiol. 2012;160:1710–8. https://doi.org/10.1104/pp.112.207753.
17. Mishra D, Shekhar S, Chakraborty S, Chakraborty N. High temperature stress responses and wheat: Impacts and alleviation strategies. Environ Exp Bot. 2021;190: 104589. https://doi.org/10.1016/j.envexpbot.2021.104589.
18. Mondal S, Karmakar S, Panda D, Pramanik K, Bose B, Singhal RK. Crucial plant processes under heat stress and tolerance through heat shock proteins. Plant Stress. 2023;10: 100227. https://doi.org/10.1016/j.stress.2023.100227.
19. Posch BC, Kariyawasam BC, Bramley H, Coast O, Richards RA, Reynolds MP, Trethowan R, Atkin OK. Exploring high temperature responses of photosynthesis and respiration to improve heat tolerance in wheat. J Exp Bot. 2019;70:5051–69. https://doi.org/10.1093/jxb/erz257.

20. Mondal S, Singh R, Crossa J, Huerta-Espino J, Sharma I, Chatrath R, Singh G, Sohu V, Mavi G, Sukuru V, Kalappanavar I, Mishra V, Hussain M, Gautam N, Uddin J, Barma N, Hakim A, Joshi A. Earliness in wheat: A key to adaptation under terminal and continual high temperature stress in South Asia. Field Crop Res. 2013;151:19–26. https://doi.org/10.1016/j.fcr.2013.06.015.
21. Pandey, A. K., Mishra, V. K., Chand, R., Navathe, S., Budhlakoti, N., Srinivasa, J., Sharma, S., & Joshi, A. K. Crosses with spelt improve tolerance of South Asian spring wheat to spot blotch, terminal heat stress, and their combination. Scientific Reports, 11 (2021). https://doi.org/10.1038/s41598-021-85238-x.
22. Mishra, D. C., Majumdar, S. G., Kumar, A., Bhati, J., Chaturvedi, K. K., Kumar, R. R., Goswami, S., Rai, A., & Budhlakoti, N. Regulatory networks of lNCRNAs, mIRNAs, and mRNAs in response to heat stress in wheat (Triticum aestivum L.): an Integrated analysis. International Journal of Genomics, (2023) 1–17. https://doi.org/10.1155/2023/1774764.
23. Chachar, Z., Fan, L., Chachar, S., Ahmed, N., Narejo, M., Ahmed, N., Lai, R., & Qi, Y. Genetic and Genomic Pathways to Improved Wheat (Triticum aestivum L.) Yields: A Review. Agronomy, 14 (2024) 1201. https://doi.org/10.3390/agronomy14061201.
24. Ćeran, M., Miladinović, D., Đorđević, V., Trkulja, D., Radanović, A., Glogovac, S., & Kondić-Špika, A. Genomics-assisted speed breeding for crop improvement: present and future. Frontiers in Sustainable Food Systems, 8 (2024). https://doi.org/10.3389/fsufs.2024.1383302.
25. Wang, S., Wong, D., Forrest, K., Allen, A., Chao, S., Huang, B. E., Maccaferri, M., Salvi, S., Milner, S. G., Cattivelli, L., Mastrangelo, A. M., Whan, A., Stephen, S., Barker, G., Wieseke, R., Plieske, J., Lillemo, M., Mather, D., Appels, R., . . . Akhunov, E. Characterization of polyploid wheat genomic diversity using a high-density 90000 single nucleotide polymorphism array. Plant Biotechnology Journal, 12 (2014) 787–796. https://doi.org/10.1111/pbi.12183.
26. Araus JL, Cairns JE. Field high-throughput phenotyping: the new crop breeding frontier. Trends Plant Sci. 2014;19:52–61. https://doi.org/10.1016/j.tplants.2013.09.008.
27. Batley J, Edwards D. Genome sequence data: management, storage, and visualization. Biotechniques. 2009;46:333–6. https://doi.org/10.2144/00011313.
28. Breseghello, F., & Sorrells, M. E. Association Mapping of Kernel Size and Milling Quality in Wheat (Triticum aestivum L.) Cultivars. Genetics, 172 (2006) 1165–1177. https://doi.org/10.1534/genetics.105.044586.
29. Liu, W., Maccaferri, M., Bulli, P., Rynearson, S., Tuberosa, R., Chen, X., & Pumphrey, M. Genome-wide association mapping for seedling and field resistance to Puccinia striiformis f. sp. tritici in elite durum wheat. Theoretical and Applied Genetics, 130 (2016) 649–667. https://doi.org/10.1007/s00122-016-2841-9.
30. Alemu SK, Huluka AB, Tesfaye K, Haileselassie T, Uauy C. Genome-wide association mapping identifies yellow rust resistance loci in Ethiopian durum wheat germplasm. PLoS ONE. 2021;16: e0243675. https://doi.org/10.1371/journal.pone.0243675.
31. Rathan, N. D., Krishna, H., Ellur, R. K., Sehgal, D., Govindan, V., Ahlawat, A. K., Krishnappa, G., Jaiswal, J. P., Singh, J. B., Sv, S., Ambati, D., Singh, S. K., Bajpai, K., & Mahendru-Singh, A. Genome-wide association study identifies loci and candidate genes for grain micronutrients and quality traits in wheat (Triticum aestivum L.). Scientific Reports, 12 (2022). https://doi.org/10.1038/s41598-022-10618-w.
32. Rahimi, Y., Khahani, B., Jamali, A., Alipour, H., Bihamta, M. R., & Ingvarsson, P. K. Genome-wide association study to identify genomic loci associated with early vigor in bread wheat under simulated water deficit complemented with quantitative trait loci meta-analysis. G3 Genes Genomes Genetics, 13 (2022). https://doi.org/10.1093/g3journal/jkac320.
33. Hao Y, Kong F, Wang L, Zhao Y, Li M, Che N, Li S, Wang M, Hao M, Zhang X, Zhao Y. Genome-wide association study of grain micronutrient concentrations in bread wheat. J Integr Agric. 2024. https://doi.org/10.1016/j.jia.2023.06.030.
34. Zhu, C., Gore, M., Buckler, E. S., & Yu, J. Status and Prospects of association mapping in plants. The Plant Genome, 1 (2008). https://doi.org/10.3835/plantgenome2008.02.0089.
35. Myles S, Peiffer J, Brown PJ, Ersoz ES, Zhang Z, Costich DE, Buckler ES. Association Mapping: Critical Considerations Shift from Genotyping to Experimental Design. Plant Cell. 2009;21:2194–202. https://doi.org/10.1105/tpc.109.068437.
36. Tello J, Ibáñez J. Review: Status and prospects of association mapping in grapevine. Plant Sci. 2023;327: 111539. https://doi.org/10.1016/j.plantsci.2022.111539.
37. Cortes, L. T., Zhang, Z., & Yu, J. Status and prospects of genome-wide association studies in plants. The Plant Genome, 14 (2021). https://doi.org/10.1002/tpg2.20077.
38. Wang, S., Feng, J., Ren, W., Huang, B., Zhou, L., Wen, Y., Zhang, J., Dunwell, J. M., Xu, S., & Zhang, Y. Improving power and accuracy of genome-wide association studies via a multi-locus mixed linear model methodology. Scientific Reports, 6 (2016). https://doi.org/10.1038/srep19444.
39. Tamba, C. L., & Zhang, Y. (2018). A fast mrMLM algorithm for multi-locus genome-wide association studies. bioRxiv (Cold Spring Harbor Laboratory). https://doi.org/10.1101/341784.
40. Wen Y, Zhang H, Ni Y, Huang B, Zhang J, Feng J, Wang S, Dunwell JM, Zhang Y, Wu R. Methodological implementation of mixed linear models in multi-locus genome-wide association studies. Brief Bioinform. 2017;19:700–12. https://doi.org/10.1093/bib/bbw145.
41. Ren W, Wen Y, Dunwell JM, Zhang Y. pKWmEB: integration of Kruskal-Wallis test with empirical Bayes under polygenic background control for multi-locus genome-wide association study. Heredity. 2017;120:208–18. https://doi.org/10.1038/s41437-017-0007-4.
42. Zhang J, Feng J, Ni Y, Wen Y, Niu Y, Tamba CL, Yue C, Song Q, Zhang Y. pLARmEB: integration of least angle regression with empirical Bayes for multilocus genome-wide association studies. Heredity. 2017;118:517–24. https://doi.org/10.1038/hdy.2017.8.
43. Tamba CL, Ni Y, Zhang Y. Iterative sure independence screening EM-Bayesian LASSO algorithm for multi-locus genome-wide association studies. PLoS Comput Biol. 2017;13: e1005357. https://doi.org/10.1371/journal.pcbi.1005357.
44. Gahlaut, V., Jaiswal, V., Singh, S., Balyan, H. S., & Gupta, P. K. Multi-Locus Genome Wide Association Mapping for Yield and Its Contributing Traits in Hexaploid Wheat under Different Water Regimes. Scientific Reports, 9 (2019). https://doi.org/10.1038/s41598-019-55520-0.
45. Vikas, V. K., Pradhan, A. K., Budhlakoti, N., Mishra, D. C., Chandra, T., Bhardwaj, S. C., Kumar, S., Sivasamy, M., Jayaprakash, P., Nisha, R., Shajitha, P., Peter, J., Geetha, M., Mir, R. R., Singh, K., & Kumar, S. Multi-locus genome-wide association studies (ML-GWAS) reveal novel genomic regions associated with seedling and adult plant stage leaf rust resistance in bread wheat (Triticum aestivum L.). Heredity, 128 (2022) 434–449. https://doi.org/10.1038/s41437-022-00525-1.
46. Osorio-Guarin, J. A., Higgins, J., Toloza-Moreno, D. L., Di Palma, F., Valencia, A. L. E., Munévar, F. R., De Vega, J. J., & Yockteng, R. Genome-wide association analyses using multi-locus models on bananas (Musa spp.) reveal candidate genes related to morphology, fruit quality, and yield. G3 Genes Genomes Genetics (2024). https://doi.org/10.1093/g3journal/jkae108.
47. Adeniyi OO, Medugorac I, Grochowska E, Düring R, Lühken G. Single-Locus and Multi-Locus Genome-Wide Association Studies Identify Genes Associated with Liver Cu Concentration in Merinoland Sheep. Genes. 2023;14:1053. https://doi.org/10.3390/genes14051053.
48. Sachdeva, S., Singh, R., Maurya, A., Singh, V. K., Singh, U. M., Kumar, A., & Singh, G. P. Multi-model genome-wide association studies for appearance quality in rice. Frontiers in Plant Science, 14 (2024). https://doi.org/10.3389/fpls.2023.1304388.
49. Kumar, S., Kumari, J., Bhusal, N., Pradhan, A. K., Budhlakoti, N., Mishra, D. C., Chauhan, D., Kumar, S., Singh, A. K., Reynolds, M., Singh, G. P., Singh, K., & Sareen, S. Genome-Wide Association study reveals genomic regions associated with ten agronomical traits in wheat under Late-Sown conditions. Frontiers in Plant Science, 11 (2020). https://doi.org/10.3389/fpls.2020.549743.
50. Rasheed A, Wen W, Gao F, Zhai S, Jin H, Liu J, Guo Q, Zhang Y, Dreisigacker S, Xia X, He Z. Development and validation of KASP assays for genes underpinning key economic traits in bread wheat. Theor Appl Genet. 2016;129:1843–60. https://doi.org/10.1007/s00122-016-2743-x.
51. Sukumaran S, Lopes M, Dreisigacker S, Reynolds M. Genetic analysis of multi-environmental spring wheat trials identifies genomic regions for locus-specific trade-offs for grain weight and grain number. Theor Appl Genet. 2017;131:985–98. https://doi.org/10.1007/s00122-017-3037-7.

52. Rehman, S. U., Sher, M. A., Saddique, M. a. B., Ali, Z., Khan, M. A., Mao, X., Irshad, A., Sajjad, M., Ikram, R. M., Naeem, M., & Jing, R. Development and exploitation of KASP assays for genes underpinning drought tolerance among wheat cultivars from Pakistan. Frontiers in Genetics, 12 (2021a). https://doi.org/10.3389/fgene.2021.684702.
53. Sandhu N, Singh J, Singh G, Sethi M, Singh MP, Pruthi G, Raigar OP, Kaur R, Kaur R, Sarao PS, Lore JS, Singh UM, Dixit S, Sagare DB, Singh S, Satturu V, Singh VK, Kumar A. Development and validation of a novel core set of KASP markers for the traits improving grain yield and adaptability of rice under direct-seeded cultivation conditions. Genomics. 2022;114:110269. https://doi.org/10.1016/j.ygeno.2022.110269.
54. Semagn K, Babu R, Hearne S, Olsen M. Single nucleotide polymorphism genotyping using Kompetitive Allele Specific PCR (KASP): overview of the technology and its application in crop improvement. Mol Breeding. 2013;33:1–14. https://doi.org/10.1007/s11032-013-9917-x.
55. Wu J, Wang Q, Kang Z, Liu S, Li H, Mu J, Dai M, Han D, Zeng Q, Chen X. Development and validation of KASP-SNP markers for QTL Underlying Resistance to stripe rust in common wheat cultivar P10057. Plant Dis. 2017;101:2079–87. https://doi.org/10.1094/pdis-04-17-0468-re.
56. Kumar, S., Pradhan, A. K., Kumar, U., Dhillon, G. S., Kaur, S., Budhlakoti, N., Mishra, D. C., Singh, A. K., Singh, R., Kumari, J., Kumaran, V. V., Mishra, V. K., Bhati, P. K., Das, S., Chand, R., Singh, K., & Kumar, S. Validation of Novel spot blotch disease resistance alleles identified in unexplored wheat (Triticum aestivum L.) germplasm lines through KASP markers. BMC Plant Biology, 22 (2022). https://doi.org/10.1186/s12870-022-04013-w.
57. Pradhan AK, Budhlakoti N, Mishra DC, Prasad P, Bhardwaj SC, Sareen S, Sivasamy M, Jayaprakash P, Geetha M, Nisha R, Shajitha P, Peter J, Kaur A, Kaur S, Vikas VK, Singh K, Kumar S. Identification of novel QTLs/Defense genes in spring wheat germplasm panel for seedling and adult plant resistance to stem rust and their validation through KASP marker assays. Plant Dis. 2023;107:1847–60. https://doi.org/10.1094/pdis-09-22-2242-re.
58. Sandhu, N., Singh, J., Ankush, A. P., Augustine, G., Raigar, O. P., Verma, V. K., Pruthi, G., & Kumar, A. Development of novel KASP markers for improved germination in Deep-Sown direct seeded rice. Rice, 17 (2024). https://doi.org/10.1186/s12284-024-00711-1.
59. Pask, AJD., Pietragalla,J., Mullan, D.M., and Reynolds, MP Physiological Breeding II: A Field Guide to Wheat Phenotyping. Mexico, D.F. (2012): CIMMYT.
60. Yan W, Kang MS. GGE Biplot Analysis. In CRC Press eBooks. 2002. https://doi.org/10.1201/9781420040371.
61. Yan W, Tinker NA. Biplot analysis of multi-environment trial data: Principles and applications. Can J Plant Sci. 2006;86:623–45. https://doi.org/10.4141/p05-169.
62. Gilmour AR, Thompson R, Cullis BR. Average Information REML: an efficient algorithm for variance parameter estimation in linear mixed models. Biometrics. 1995;51:1440. https://doi.org/10.2307/2533274.
63. Doyle JJ. Isolation of plant DNA from fresh tissue. Focus. 1990;12:13–5.
64. Pritchard JK, Stephens M, Donnelly P. Inference of population structure using multilocus genotype data. Genetics. 2000;155:945–59. https://doi.org/10.1093/genetics/155.2.945.
65. Evanno G, Regnaut S, Goudet J. Detecting the number of clusters of individuals using the software structure: a simulation study. Mol Ecol. 2005;14:2611–20. https://doi.org/10.1111/j.1365-294x.2005.02553.x.
66. Duncan O, Trösch J, Fenske R, Taylor NL, Millar AH. Resource: Mapping the Triticum aestivum proteome. Plant J. 2017;89:601–16. https://doi.org/10.1111/tpj.1340.
67. Bradbury PJ, Zhang Z, Kroon DE, Casstevens TM, Ramdoss Y, Buckler ES. TASSEL: software for association mapping of complex traits in diverse samples. Bioinformatics. 2007;23(19):2633–5. https://doi.org/10.1093/bioinformatics/btm308.
68. Kruskal WH, Wallis WA. Use of ranks in One-Criterion variance analysis. J Am Stat Assoc. 1952;47:583. https://doi.org/10.2307/2280779.
69. Chauhan H, Khurana N, Nijhavan A, Khurana JP, Khurana P. The wheat chloroplastic small heat shock protein (sHSP26) is involved in seed maturation and germination and imparts tolerance to heat stress. Plant, Cell Environ. 2012;35:1912–31. https://doi.org/10.1111/j.1365-3040.2012.02525.x.
70. Yadav, S., Rathore, M. S., & Mishra, A. The Pyruvate-Phosphate Dikinase (C4-SmPPDK) Gene From Suaeda monoica Enhances Photosynthesis, Carbon Assimilation, and Abiotic Stress Tolerance in a C3 Plant Under Elevated CO2 Conditions. Frontiers in Plant Science, 11 (2020). https://doi.org/10.3389/fpls.2020.00345.
71. Hoang, X. L. T., Nhi, D. N. H., Thu, N. B. A., Thao, N. P., & Tran, L. P. Transcription Factors and Their Roles in Signal Transduction in Plants under Abiotic Stresses. Current Genomics, 18 (2017). https://doi.org/10.2174/1389202918666170227150057.
72. Opassiri, R., Pomthong, B., Onkoksoong, T., Akiyama, T., Esen, A., & Cairns, J. R. K. Analysis of rice glycosyl hydrolase family 1 and expression of Os4bglu12 β-glucosidase. BMC Plant Biology, 6 (2006). https://doi.org/10.1186/1471-2229-6-33.
73. Liu, H., Hu, M., Wang, Q., Cheng, L., & Zhang, Z. Role of Papain-Like cysteine proteases in plant development. Frontiers in Plant Science, 9 (2018). https://doi.org/10.3389/fpls.2018.01717.
74. Won, K., & Kim, H. Functions of the plant QBC SNARE SNAP25 in cytokinesis and biotic and abiotic stress responses. Molecules and Cells, 43 (2020) 313–322. https://doi.org/10.14348/molcells.2020.2245.
75. Dong N, Chen L, Ahmad S, Cai Y, Duan Y, Li X, Liu Y, Jiao G, Xie L, Hu S, Sheng Z, Shao G, Wang L, Tang S, Wei X, Hu P. Genome-Wide analysis and functional characterization of pyruvate kinase (PK) gene family modulating rice yield and quality. Int J Mol Sci. 2022;23:15357. https://doi.org/10.3390/ijms232315357.
76. Guerin, C., Roche, J., Allard, V., Ravel, C., Mouzeyar, S., & Bouzidi, M. F. Genome-wide analysis, expansion and expression of the NAC family under drought and heat stresses in bread wheat (T. aestivum L.). PLOS ONE, 14 (2019) e0213390. https://doi.org/10.1371/journal.pone.0213390.
77. Jiang S, Meng B, Zhang Y, Li N, Zhou L, Zhang X, Xu R, Guo S, Song C, Li Y. An SNW/SKI-INTERACTING PROTEIN influences endoreduplication and cell growth in Arabidopsis. Plant Physiol. 2022;190:2217–28. https://doi.org/10.1093/plphys/kiac415.
78. Matsushima N, Miyashita H. Leucine-Rich repeat (LRR) domains containing intervening motifs in plants. Biomolecules. 2012;2:288–311. https://doi.org/10.3390/biom2020288.
79. Han Y, Gao Y, Li Y, Zhai X, Zhou H, Ding Q, Ma L. Chloroplast genes are involved in the Male-Sterility of K-Type CMS in wheat. Genes. 2022;13:310. https://doi.org/10.3390/genes13020310.
80. Hayat S, Hayat Q, Alyemeni MN, Wani AS, Pichtel J, Ahmad A. Role of proline under changing environments. Plant Signal Behav. 2012;7:1456–66. https://doi.org/10.4161/psb.21949.
81. Díaz-Mendoza, M., DíAz, I., & Martínez, M. Insights on the proteases involved in barley and wheat grain germination. International Journal of Molecular Sciences, 20 (2019) 2087. https://doi.org/10.3390/ijms20092087.
82. Liang Q, Wang K, Liu X, Riaz B, Ling J, Wan X, Ye X, Zhang C. Improved folate accumulation in genetically modified maize and wheat. J Exp Bot. 2019;70:1539–51. https://doi.org/10.1093/jxb/ery453.
83. Hajiahmadi, Z., Abedi, A., Wei, H., Sun, W., Ruan, H., Zhuge, Q., & Movahedi, A. Identification, evolution, expression, and docking studies of fatty acid desaturase genes in wheat (Triticum aestivum L.). BMC Genomics, 21 (2020). https://doi.org/10.1186/s12864-020-07199-1.
84. Lai Y, Zhang D, Wang J, Wang J, Ren P, Yao L, Si E, Kong Y, Wang H. Integrative Transcriptomic and Proteomic Analyses of Molecular Mechanism Responding to Salt Stress during Seed Germination in Hulless Barley. Int J Mol Sci. 2020;21:359. https://doi.org/10.3390/ijms21010359.
85. Jiang, X., Zhou, W., Li, D., Wang, H., Yang, Y., You, J., Liu, H., Ai, L., & Zhang, M. Combined transcriptome and metabolome analyses reveal the effects of selenium on the growth and quality of Lilium lancifolium. Frontiers in Plant Science, 15 (2024). https://doi.org/10.3389/fpls.2024.1399152.
86. Khalid, A., Hameed, A., & Tahir, M. F. Wheat quality: A review on chemical composition, nutritional attributes, grain anatomy, types, classification, and function of seed storage proteins in bread making quality. Frontiers in Nutrition, 10 (2023). https://doi.org/10.3389/fnut.2023.1053196.
87. Trethowan, R. M. Abiotic stresses. In Springer eBooks (2022) 159–175. https://doi.org/10.1007/978-3-030-90673-3_10.
88. Mao H, Jiang C, Tang C, Nie X, Du L, Liu Y, Cheng P, Wu Y, Liu H, Kang Z, Wang X. Wheat adaptation to environmental stresses under climate change: Molecular basis and genetic improvement. Mol Plant. 2023;16:1564–89. https://doi.org/10.1016/j.molp.2023.09.001.

89. Kumar, H., Chugh, V., Kumar, M., Gupta, V., Prasad, S., Kumar, S., Singh, C. M., Kumar, R., Singh, B. K., Panwar, G., & Kumar, M. Investigating the impact of terminal heat stress on contrasting wheat cultivars: a comprehensive analysis of phenological, physiological, and biochemical traits. Frontiers in Plant Science, 14 (2023). https://doi.org/10.3389/fpls.2023.1189005.
90. Molero, G., Coombes, B., Joynson, R., Pinto, F., Piñera-Chávez, F. J., Rivera-Amado, C., Hall, A., & Reynolds, M. P. Exotic alleles contribute to heat tolerance in wheat under field conditions. Communications Biology, 6 (2023). https://doi.org/10.1038/s42003-022-04325-5.
91. Berkman PJ, Lai K, Lorenc MT, Edwards D. Next-generation sequencing applications for wheat crop improvement. Am J Bot. 2012;99:365–71. https://doi.org/10.3732/ajb.110030.
92. Lopes MS, El-Basyoni I, Baenziger PS, Singh S, Royo C, Ozbek K, Aktas H, Ozer E, Ozdemir F, Manickavelu A, Ban T, Vikram P. Exploiting genetic diversity from landraces in wheat breeding for adaptation to climate change. J Exp Bot. 2015;66:3477–86. https://doi.org/10.1093/jxb/erv122.
93. Mu H, Wang B, Yuan F. Bioinformatics in plant breeding and research on disease resistance. Plants. 2022;11(22):3118. https://doi.org/10.3390/plants11223118.
94. Rabieyan, E., Bihamta, M. R., Moghaddam, M. E., Mohammadi, V., & Alipour, H. Genome-wide association mapping for wheat morphometric seed traits in Iranian landraces and cultivars under rain-fed and well-watered conditions. Scientific Reports, 12 (2022). https://doi.org/10.1038/s41598-022-22607-0.
95. Wang J, Cheng J, Sun D. Enhancement of wheat seed germination, seedling growth and nutritional properties of wheat plantlet juice by plasma activated water. J Plant Growth Regul. 2022;42:2006–22. https://doi.org/10.1007/s00344-022-10677-3.
96. Kaya, Y. Phenotyping winter wheat for early ground cover. Czech Journal of Genetics and Plant Breeding, 58 (2022) 189–200. https://doi.org/10.17221/91/2021-cjgpb.
97. Scavo, A., Fontanazza, S., Restuccia, A., Pesce, G. R., Abbate, C., & Mauromicale, G. The role of cover crops in improving soil fertility and plant nutritional status in temperate climates. A review. Agronomy for Sustainable Development, 42 (2022). https://doi.org/10.1007/s13593-022-00825-0.
98. Silva GC, Bagavathiannan M. Mechanisms of weed suppression by cereal rye cover crop: A review. Agron J. 2023;115:1571–85. https://doi.org/10.1002/agj2.21347.
99. Rehman HU, Tariq A, Ashraf I, Ahmed M, Muscolo A, Basra SMA, Reynolds M. Evaluation of physiological and morphological traits for improving spring wheat adaptation to terminal heat stress. Plants. 2021;10:455. https://doi.org/10.3390/plants10030455.
100. Sattar, A., Nanda, G., Singh, G., Jha, R. K., & Bal, S. K. Responses of phenology, yield attributes, and yield of wheat varieties under different sowing times in Indo-Gangetic Plains. Frontiers in Plant Science, 14 (2023). https://doi.org/10.3389/fpls.2023.1224334.
101. Cann DJ, Hunt JR, Porker KD, Harris FA, Rattey A, Hyles J. The role of phenology in environmental adaptation of winter wheat. Eur J Agron. 2023;143: 126686. https://doi.org/10.1016/j.eja.2022.126686.
102. Niu Y, Chen T, Zhao C, Zhou M. Improving crop lodging resistance by adjusting plant height and stem strength. Agronomy. 2021;11:2421. https://doi.org/10.3390/agronomy11122421.
103. Miao L, Wang X, Yu C, Ye C, Yan Y, Wang H. What factors control plant height?1. J Integr Agric. 2024;23:1803–24. https://doi.org/10.1016/j.jia.2024.03.058.
104. Vicentin, L., Canales, J., & Calderini, D. F. The trade-off between grain weight and grain number in wheat is explained by the overlapping of the key phases determining these major yield components. Frontiers in Plant Science, 15 (2024). https://doi.org/10.3389/fpls.2024.1380429.
105. Liao, S., Xu, Z., Fan, X., Zhou, Q., Liu, X., Jiang, C., Chen, L., Lin, D., Feng, B., & Wang, T. Genetic dissection and validation of a major QTL for grain weight on chromosome 3B in bread wheat (Triticum aestivum L.). Journal of Integrative Agriculture, 23 (2024) 77–92. https://doi.org/10.1016/j.jia.2023.04.023.
106. Gozdowski D, Stępień M, Panek E, Varghese J, Bodecka E, Rozbicki J, Samborski S. Comparison of winter wheat NDVI data derived from Landsat 8 and active optical sensor at field scale. Remote Sensing Applications Society and Environment. 2020;20: 100409. https://doi.org/10.1016/j.rsase.2020.100409.
107. Barboza, T. O. C., Ardigueri, M., Souza, G. F. C., Ferraz, M. a. J., Gaudencio, J. R. F., & Santos, A. F. D. Performance of vegetation indices to estimate green biomass accumulation in common bean. AgriEngineering, 5 (2023) 840–854. https://doi.org/10.3390/agriengineering5020052.
108. Lepekhov, S. B. Canopy temperature depression for droughtand heat stress tolerance in wheat breeding. Vavilov Journal of Genetics and Breeding, 26 (2022) 196–201. https://doi.org/10.18699/vjgb-22-24.
109. Hatfield JL, Prueger JH. Temperature extremes: Effect on plant growth and development. Weather and Climate Extremes. 2015;10:4–10. https://doi.org/10.1016/j.wace.2015.08.001.
110. Zhao K, Tao Y, Liu M, Yang D, Zhu M, Ding J, Zhu X, Guo W, Zhou G, Li C. Does temporary heat stress or low temperature stress similarly affect yield, starch, and protein of winter wheat grain during grain filling? J Cereal Sci. 2022;103: 103408. https://doi.org/10.1016/j.jcs.2021.103408.
111. Bishwas KC, Poudel MR, Regmi D. AMMI and GGE biplot analysis of yield of different elite wheat line under terminal heat stress and irrigated environments. Heliyon. 2021;7(6): e07206. https://doi.org/10.1016/j.heliyon.2021.e07206.
112. Gupta V, Mehta G, Kumar S, Ramadas S, Tiwari R, Singh GP, Sharma P. AMMI and GGE biplot analysis of yield under terminal heat tolerance in wheat. Mol Biol Rep. 2023;50:3459–67. https://doi.org/10.1007/s11033-023-08298-4.
113. Wang, L., Xu, J., Wang, H., Chen, T., You, E., Bian, H., Chen, W., Zhang, B., & Shen, Y. Population structure analysis and genome-wide association study of a hexaploid oat landrace and cultivar collection. Frontiers in Plant Science, 14 (2023). https://doi.org/10.3389/fpls.2023.1131751.
114. Jo, K. R., Cho, S., Cho, J., Park, H., Choi, J., Park, Y., & Cho, K. Analysis of genetic diversity and population structure among cultivated potato clones from Korea and global breeding programs. Scientific Reports, 12 (2022). https://doi.org/10.1038/s41598-022-12874-2.
115. Kimwemwe, P. K., Bukomarhe, C. B., Mamati, E. G., Githiri, S. M., Civava, R. M., Mignouna, J., Kimani, W., & Fofana, M. Population Structure and Genetic Diversity of Rice (Oryza sativa L.) Germplasm from the Democratic Republic of Congo (DRC) Using DArTseq-Derived Single Nucleotide Polymorphism (SNP). Agronomy, 13 (2023) 1906. https://doi.org/10.3390/agronomy13071906.
116. Dube, S. P., Sibiya, J., & Kutu, F. Genetic diversity and population structure of maize inbred lines using phenotypic traits and single nucleotide polymorphism (SNP) markers. Scientific Reports, 13 (2023). https://doi.org/10.1038/s41598-023-44961-3.
117. Atsbeha, G., Tesfaye, K., Mekonnen, T., Haileselassie, T., & Kebede, M. (2023). Genetic diversity and population structure analysis of bread wheat (Triticum aestivum L.) germplasms as revealed by inter simple sequence repeat (ISSR) markers. Genetic Resources and Crop Evolution. https://doi.org/10.1007/s10722-023-01791-6.
118. Platt, A., Horton, M., Huang, Y. S., Li, Y., Anastasio, A. E., Mulyati, N. W., Ågren, J., Bossdorf, O., Byers, D., Donohue, K., Dunning, M., Holub, E. B., Hudson, A., Corre, V. L., Loudet, O., Roux, F., Warthmann, N., Weigel, D., Rivero, L., . . . Borevitz, J. O. The Scale of Population Structure in Arabidopsis thaliana. PLoS Genetics, 6 (2010) e1000843. https://doi.org/10.1371/journal.pgen.1000843.
119. Hunt, H. V., Przelomska, N. a. S., Campana, M. G., Cockram, J., Bligh, H. F. J., Kneale, C. J., Romanova, O. I., Malinovskaya, E. V., & Jones, M. K. Population genomic structure of Eurasian and African foxtail millet landrace genotypes inferred from genotyping-by-sequencing. The Plant Genome, 14 (2021). https://doi.org/10.1002/tpg2.20081.
120. Dadshani, S., Mathew, B., Ballvora, A., Mason, A. S., & Léon, J. Detection of breeding signatures in wheat using a linkage disequilibrium-corrected mapping approach. Scientific Reports, 11 (2021). https://doi.org/10.1038/s41598-021-85226-1.
121. Flint-Garcia SA, Thuillet A, Yu J, Pressoir G, Romero SM, Mitchell SE, Doebley J, Kresovich S, Goodman MM, Buckler ES. Maize association population: a high-resolution platform for quantitative trait locus dissection. Plant J. 2005;44:1054–64. https://doi.org/10.1111/j.1365-313x.2005.02591.x.
122. Roncallo, P. F., Larsen, A. O., Achilli, A. L., Pierre, C. S., Gallo, C. A., Dreisigacker, S., & Echenique, V. Linkage disequilibrium patterns, population structure and diversity analysis in a worldwide durum wheat collection including Argentinian genotypes. BMC Genomics, 22 (2021). https://doi.org/10.1186/s12864-021-07519-z.

123. Pang, Y., Liu, C., Wang, D., St Amand, P., Bernardo, A., Li, W., He, F., Li, L., Wang, L., Yuan, X., Dong, L., Su, Y., Zhang, H., Zhao, M., Liang, Y., Jia, H., Shen, X., Lu, Y., Jiang, H., . . . Liu, S. High-Resolution Genome-Wide Association study identifies genomic regions and candidate genes for important agronomic traits in wheat. Molecular Plant, 13 (2020) 1311–1327. https://doi.org/10.1016/j.molp.2020.07.008.
124. Devate, N. B., Krishna, H., Parmeshwarappa, S. K. V., Manjunath, K. K., Chauhan, D., Singh, S., Singh, J. B., Kumar, M., Patil, R., Khan, H., Jain, N., Singh, G. P., & Singh, P. K. Genome-wide association mapping for component traits of drought and heat tolerance in wheat. Frontiers in Plant Science, 13 (2022). https://doi.org/10.3389/fpls.2022.943033.
125. Butler, J. B., Freeman, J. S., Potts, B. M., Vaillancourt, R. E., Kahrood, H. V., Ades, P. K., Rigault, P., & Tibbits, J. F. G. Patterns of genomic diversity and linkage disequilibrium across the disjunct range of the Australian forest tree Eucalyptus globulus. Tree Genetics & Genomes, 18 (2022). https://doi.org/10.1007/s11295-022-01558-7.
126. Zhang, Y., Jia, Z., & Dunwell, J. M. Editorial: The Applications of New Multi-Locus GWAS Methodologies in the Genetic Dissection of Complex Traits. Frontiers in Plant Science, 10 (2019). https://doi.org/10.3389/fpls.2019.00100.
127. Chaurasia, S., Singh, A. K., Songachan, L., Sharma, A. D., Bhardwaj, R., & Singh, K. Multi-locus genome-wide association studies reveal novel genomic regions associated with vegetative stage salt tolerance in bread wheat (Triticum aestivum L.). Genomics, 112 (2020) 4608–4621. https://doi.org/10.1016/j.ygeno.2020.08.006.
128. Pinto RS, Reynolds MP, Mathews KL, McIntyre CL, Olivares-Villegas J, Chapman SC. Heat and drought adaptive QTL in a wheat population designed to minimize confounding agronomic effects. Theor Appl Genet. 2010;121:1001–21. https://doi.org/10.1007/s00122-010-1351-4.
129. Bennett, D., Reynolds, M., Mullan, D., Izanloo, A., Kuchel, H., Langridge, P., & Schnurbusch, T. Detection of two major grain yield QTL in bread wheat (Triticum aestivum L.) under heat, drought and high yield potential environments. Theoretical and Applied Genetics, 125 (2012) 1473–1485. https://doi.org/10.1007/s00122-012-1927-2.
130. Chen, W., Sun, D., Li, R., Wang, S., Shi, Y., Zhang, W., & Jing, R. Mining the stable quantitative trait loci for agronomic traits in wheat (Triticum aestivum L.) based on an introgression line population. BMC Plant Biology, 20 (2020). https://doi.org/10.1186/s12870-020-02488-z.
131. Ding, Y., Fang, H., Gao, Y., Fan, G., Shi, X., Yu, S., Ding, S., Huang, T., Wang, W., & Song, J. Genome-wide association analysis of time to heading and maturity in bread wheat using 55K microarrays. Frontiers in Plant Science, 14 (2023). https://doi.org/10.3389/fpls.2023.1296197.
132. Cerit, M., Wang, Z., Dogan, M., Yu, S., Valenzuela-Antelo, J. L., Chu, C., Wang, S., Xue, Q., Ibrahim, A. M. H., Rudd, J. C., Metz, R., Johnson, C. D., & Liu, S. Mapping QTL for Yield and Its Component Traits Using Wheat (Triticum aestivum L.) RIL Mapping Population from TAM 113 × Gallagher. Agronomy, 13(2023) 2402. https://doi.org/10.3390/agronomy13092402.
133. Peng J, Richards DE, Hartley NM, Murphy GP, Devos KM, Flintham JE, Beales J, Fish LJ, Worland AJ, Pelica F, Sudhakar D, Christou P, Snape JW, Gale MD, Harberd NP. 'Green revolution' genes encode mutant gibberellin response modulators. Nature. 1999;400:256–61. https://doi.org/10.1038/22307.
134. Yu, M., Liu, Z., Yang, B., Chen, H., Zhang, H., & Hou, D. The contribution of photosynthesis traits and plant height components to plant height in wheat at the individual quantitative trait locus level. Scientific Reports, 10 (2020). https://doi.org/10.1038/s41598-020-69138-0.
135. Cheng B, Gao X, Luo Y, Ding Y, Chen T, Cao N, Xu J, Xin Z, Zhang L. Utilization of wheat 55K SNP array for QTL mapping of plant height and flag leaf in a RIL population. Cereal Research Communications. 2023. https://doi.org/10.1007/s42976-023-00475-2.
136. Jamil, M., Ali, A., Gul, A., Ghafoor, A., Napar, A. A., Ibrahim, A. M. H., Naveed, N. H., Yasin, N. A., & Mujeeb-Kazi, A. Genome-wide association studies of seven agronomic traits under two sowing conditions in bread wheat. BMC Plant Biology, 19 (2019). https://doi.org/10.1186/s12870-019-1754-6.
137. Zahra N, Wahid A, Hafeez MB, Ullah A, Siddique KH, Farooq M. Grain development in wheat under combined heat and drought stress: Plant responses and management. Environ Exp Bot. 2021;188: 104517. https://doi.org/10.1016/j.envexpbot.2021.104517.
138. Guan, P., Lu, L., Jia, L., Kabir, M. R., Zhang, J., Lan, T., Zhao, Y., Xin, M., Hu, Z., Yao, Y., Ni, Z., Sun, Q., & Peng, H. Global QTL Analysis Identifies Genomic Regions on Chromosomes 4A and 4B Harboring Stable Loci for Yield-Related Traits Across Different Environments in Wheat (Triticum aestivum L.). Frontiers in Plant Science, 9 (2018). https://doi.org/10.3389/fpls.2018.00529.
139. Zhang, H., Bao, Y., Li, X., Feng, D., & Wang, H. QTL mapping for 1000-grain weight and its main components in wheat. Research Square (2021). https://doi.org/10.21203/rs.3.rs-490169/v1.
140. Duhan, N., Panigrahi, S., Pal, N., Saini, D. K., Balyan, P., Singh, Y., Mir, R. R., Singh, K. P., Kumar, S., Dhankher, O. P., & Kumar, U. Identification and expression analysis of genomic regions associated with the traits contributing to lodging tolerance in wheat (Triticum aestivum L.). European Journal of Agronomy, 154 (2024) 127073. https://doi.org/10.1016/j.eja.2023.127073.

Publisher's Note